DANAE Letter of Intent

C. Biscari, D. Alesini, R. Bedogni, M.E. Biagini, R. Boni, M. Boscolo, B. Buonomo,
M. Calvetti, M. Castellano, A. Clozza, G.O. Delle Monache, E. Di Pasquale, G. Di Pirro,
A. Drago, A. Esposito, L. Falbo, A. Gallo, A. Ghigo, S. Guiducci, M. Incurvati, P. Iorio,
C. Ligi, F. Marcellini, C. Marchetti, G. Mazzitelli, C. Milardi, L. Pellegrino, M.A. Preger,
L. Quintieri, U. Rotundo, R. Ricci, C. Sanelli, M. Serio, F. Sgamma, B. Spataro,
A. Stecchi, A. Stella, S. Tomassini, C. Vaccarezza, M. Zobov, *INFN-LNF, Frascati, Italy*

E.B.Levichev, N.A.Mezentsev, S.A.Nikitin, P.A.Piminov, D.N.Shatilov,
P.D.Vobly, *BINP, Novosibirsk, Russia*

B. Parker, *BNL, Brookhaven, USA*

J. Fox, D. Teytelman, *SLAC, Stanford, USA*

INTRODUCTION

Lepton factories based on double storage rings and high frequency collisions of flat beams were designed in the 1990s, and came to operation just before the end of last century. The Φ-factory in Italy, DAΦNE [1] and the two B-factories on opposite sides of the Pacific Ocean, KEKB [2] in Japan and PEPII [3] in USA, are planning the end of their operations after almost one decade of operation, while waiting for the first beams of the new factories, BEPCII [4], the Chinese tau-charm at Beijing, and VEPP-2000 [5], the first collider based on round beam collisions, in Novosibirsk. The future upgrades after 2010 of the two B-factories and of the Phi-factory are the subjects of discussions in the flavour physics communities.

In Frascati the DAΦNE original physics program, ranging from K-meson to nuclear and atomic physics, will be completed well before 2010, when the three experiments, KLOE [6], FINUDA [7] and DEAR [8], will collect the required statistics. Interest in pursuing further these three research fields, together with a wider particle physics program, including $\gamma-\gamma$ experiments, has shown up and is described in separated documents [9-12]. The proposed experiments at the Φ are more demanding in terms of luminosity with respect to the present DAΦNE parameters, and even the foreseen collider upgrades for the next future will not fulfill completely the experimental requirements. A flexible range of energy is furthermore requested, to cover the energy span between the Φ and the tau-charm resonances.

This document describes the feasibility study of an e^+e^- collider whose range of energy and luminosity is shown in Table I. The design is site dependent since it is optimized to use DAΦNE buildings, infrastructures, injection system, and part of the ring hardware, with an overall minimization of cost and construction time.

Following the Frascati tradition of applying mythological names to its accelerators, we have called it DANAE (DAφne New with Adjustable Energy). Danaë, the daughter of the King of Argos, shut by her father in a tower with bronze doors, was visited by Zeus in the form of a shower of gold falling from a cloud, and from their union Perseus was born.

Table I – DANAE Luminosity and Energy Range

Energy in the center of mass (GeV)	1.02	2.4
Peak luminosity > ($cm^{-1}sec^{-2}$)	10^{33}	10^{32}
Total integrated luminosity ($fbarn^{-1}$)	50	3

The project excellence is assured by the application of the most recent technologies, on the basis of experience from DAΦNE and the group expertise, and by the possibility of using the next DAΦNE runs as R&D for some of the proposed new principles.

The accelerator community has recently evolved towards a phase of extended collaborations in view of the construction of large projects, like ILC [13], thanks also to the ever increasing participation of the Asian world. Even small projects like DANAE take advantage of this new attitude and several international groups participate to the collider design.

DANAE design is the final step of a process in which the possibilities to upgrade DAΦNE in energy and/or luminosity have been investigated, a process which started in the workshop held in Alghero in September 2003 [14]. Let's summarize the conclusions reached so far:

- The maximum luminosity for a Φ-factory based on present knowledge, and involving a time limited R&D is in the range of 10^{33} $cm^{-2}sec^{-1}$. Luminosity higher by one order of magnitude can be envisaged if very innovative regimes are foreseen (such as the strong RF focusing [15]), needing strong R&D effort, and not risk free. Going to still higher values is not conceivable at present even with the most imaginative accelerator designs.

- The maximum energy reachable by the DAΦNE complex with the present hardware is 750 MeV per beam. By substituting dipoles, splitters and the Interaction Region, the energy of 1 GeV per beam can be reached, not yet satisfying the experimental requirements. A preliminary evaluation of the necessary changes to reach the energy of 1.2 GeV per beam [16] has shown that the vacuum chamber and part of the magnetic elements need to be substituted. The luminosity required at the neutron-antineutron form factor threshold is in the range of 10^{32} $cm^{-2}sec^{-1}$, and does not represent a major challenge for the design, but for the particle losses, which must be kept below the allowed radiation doses, if the LNF buildings are being reused.

Summing up all above considerations we came to the design of a flexible collider, with the luminosity optimized at the Φ energy, and with the maximum reachable energy compatible with the present LNF infrastructures. The design is flexible enough to ensure the possibility of future upgrades in view of further developments in the field of collider physics, but is based on well assessed principles, in order to shorten as far as possible the time necessary for its completion.

In the following the collider design is briefly described, while the estimated cost and schedule are shown in the final paragraph.

DESIGN CRITERIA

The most demanding set of DANAE parameters corresponds to the high luminosity at the Φ-energy. The luminosity at higher energy comes almost for free once the collider hardware is correctly dimensioned.

The basic DANAE design criteria are the same adopted by all factories up to now: double ring, multibunch regime, flat beams and high collision frequency.

All factories run with a single experiment in the machine: the present DAΦNE layout has two Interaction Regions (IRs), where two experiments can be installed at the same time, but only one takes data while the other one is parked. In fact the optimization of the luminosity parameters in two collision points and background shielding on both IRs has shown to be critical, and it is more effective in terms of peak and integrated luminosity to dedicate each run to a single detector.

DANAE has therefore one single IR, where the experiments will be installed sequentially, thus leaving a long straight section opposite to the IR free, which can be used for injection, RF and feedback systems.

If the different experiments use a single detector, gain in shutdown and commissioning time is obtained. The DANAE design is based on the reutilization of the KLOE detector, with a tunable IR fitting different energies and detector solenoid field.

One of the main characteristics of the new collider is its flexibility. Beyond the two nominal sets of parameters, one corresponding to the high luminosity in the regime of Φ-factory, the second to the maximum reachable energy, the possibility of tuning the main collider parameters in a wide range is kept, with special care to the tunability of momentum compaction, emittance and betatron tunes. All quadrupoles and sextupoles will have independent power supplies following the DAΦNE approach which has proven to be very useful during machine commissioning, machine study shifts and operation.

Table II contains the list of the main parameters for the two operating conditions, compared to those of DAΦNE corresponding to the peak luminosity reached so far.

It can be remarked that the gain in luminosity with respect to the present DAΦNE parameters is based on the increase of collision frequency, thanks to the higher RF frequency, of the colliding currents, but specially of the specific luminosity.

Let's recall the luminosity expression:

$$L = \frac{f_{coll}}{2\pi} \frac{N^+ N^-}{\Sigma_x^* \Sigma_y^*} \qquad (1)$$

where

$$f_{coll} = N_b f_o \qquad (2)$$

is the collision frequency, defined by the number of bunches N_b and the revolution frequency f_o; N^+ and N^- are the number of particles per bunch and

$$\Sigma_{x,y}^* = \sqrt{\sigma_{+,x,y}^{*2} + \sigma_{-,x,y}^{*2}} \qquad (3)$$

are the beam cross sections at the Interaction Point (IP).

Table II – DANAE design parameters as a Φ-factory and at the maximum energy, compared with DAΦNE parameters at the present peak luminosity.

		Units	DAΦNE	DANAE @ Φ	DANAE 1.2 GeV
Date			2006	16-3-2006	16-3-2006
Energy (center of mass)	E_{cm}	GeV	1.02	1.02	2.4
Energy per ring	E	GeV	0.51	0.51	1.2
Number of rings			2	2	2
Circumference	C	m	97.69	96.34	96.34
Number of IPs			1	1	1
Revolution frequency	f_{rev}	MHz	3.07	3.11	3.11
Time between collisions	Tc	nsec	2.7	2.0	6.0
Bunch spacing	s_b	m	0.81	0.60	1.80
Half crossing angle	θ/2	mrad	15	15	15
# of Colliding Bunches	N_b		110	150	30
Particles per bunch	N_{part}	(10^{10})	2-3	3	3.4
Beam current (e-/e+)	I	A	1.4/1.3	2.25	0.5
Bunch current (e-/e+)	I_b	mA	13/12	15	16.6
Peak Luminosity (10^{32})	L_{peak}	$cm^{-2}sec^{-1}$	1.5	10	> 2
Specific Luminosity/bunch (10^{28})	L_{sp}	$cm^{-2}sec^{-1}mA^{-2}$	0.9	3	3
Horizontal β function @ IP	H	m	2	1	1
Vertical β function @ IP	V	cm	1.8	0.8	1
Horizontal emittance	ε	mm mrad	0.4	0.45	0.45
Coupling factor	κ	%	1.1	0.5	0.5
Horizontal Σ in collision	Σ_x	mm	1.26	0.95	0.95
Vertical Σ in collision	Σ_y	μm	12.6	6	6.7
Horizontal Beam-beam tune shift	ξ_x		0.026	0.030	0.014
Vertical Beam-beam tune shift	ξ_y		0.025	0.038	0.020
Bunch length (e-/e+)	σ_L	cm	3/2	1	1.5
Piwinski angle*	φ		0.42	0.22	.33
Momentum compaction	α_c		0.027	0.02	0.03
Synchrotron radiation integral	I_2	m^{-1}	9.5	22.4	5.6
Synchrotron radiation integral	I_3	m^{-2}	8.5	42.6	3.6
Synchrotron radiation integral	I_4	m^{-1}	0.3	0.2	0.5
Synchrotron radiation integral	I_5	m^{-1}	9.6	23.9	1.1
Energy loss per turn	U_O	keV	9	21.4	165
Longitudinal damping time	τ_S	msec	17.9	7.6	2.2
RF frequency	f_{rf}	MHz	368.26	500	500
RF voltage (e-/e+)	V	MV	0.12/0.18	0.4	1.5
Ring impedance	Z/n	Ω	1.1/0.6	0.5	0.5
Total Beam Power	P_t	kW	45**	48	83
Wiggler beam power	P_W	kW	24**	42	43
Dipole beam power	P_d	kW	21**	6	40
Injection energy	E_{inj}	GeV	0.51	0.51	0.51

* The Piwinski angle is defined as: $\phi = \theta \sigma_L/2\sigma_x$

** These values refer to DAΦNE design for a maximum current of 5A per beam

The so called specific luminosity per bunch is defined as

$$L_{sp} = \frac{L_{bunch}}{I_b^+ I_b^-}$$ (4)

Keeping the beam cross section small in collision at high currents is the key point of the high luminosity regime. Let's now mention briefly the considerations on which we base our nominal set of parameters.

In a flat beam collider the beam size at the IP is minimized by the smallest achievable vertical β* compatible with chromaticity contribution and especially with bunch length: the bunch length should be comparable or slightly longer than β^*, otherwise the luminosity decreases very fast due to the geometric "hourglass effect" and beam-beam synchro-betatron resonances.

The bunch design current should not exceed too much the threshold current of the longitudinal microwave instability in order to avoid the drawbacks which appear above the threshold. The MI threshold is given by [17]:

$$I_{th} = \sqrt{2\pi} \; \frac{\alpha_c (E/e)(\sigma_E/E)^2 \sigma_l}{|Z/n| R}$$ (5)

where the natural energy spread is:

$$\frac{\sigma_E^2}{E^2} = C_q \gamma^2 \frac{I_3}{I_2 + I_4}$$ (6)

with $C_q = \dfrac{55}{32\sqrt{3}} \dfrac{hc}{2\pi mc^2} = 3.8319 \cdot 10^{-13} \, m$

I_j are the synchrotron radiation integrals [18] and $Z_{||}/n$ is the ring impedance.

The first phenomenon is the bunch length and energy spread growing with the product of the bunch current and the ring impedance. A correlated vertical size blow up has also been observed at DAΦNE [19].

Other effects are the coherent oscillations inside the bunch like the "saw-tooth" oscillations seen at SLAC damping ring [20] or the "quadrupole mode instability" in the DAΦNE electron ring [21]. Such oscillations in collisions lead to beam lifetime reduction, luminosity decrease and excessive background in the detector.

It is clear that the impedance minimization of all elements of the vacuum chamber is of extreme importance, both to increase I_{th} and to decrease the strength of the instability. Experience in the DAΦNE vacuum chamber design, which has obtained the minimum ring impedance for such short machines (0.6 Ω for the positron ring and twice as much for the electron one, the difference due to the presence of long ion clearing electrodes, ICE) will be of great help.

The longitudinal synchrotron tune Q_s should not be too high. This has been confirmed by the dedicated measurements at CESR of the luminosity versus the synchrotron tune [22] and has been also verified in numerical simulations of the beam-beam effects for DANAE.

The emittance is chosen by finding the best compromise between two different effects: a high value is positive from the point of view of beam-beam tune shift, a low one is better from the point of view of parasitic crossings and small cross section at collision.

The radiation damping increase is beneficial for several reasons, first of all the shorter damping time, which interferes with the beam-beam behavior and with all instabilities with risetimes in the range of msec, including the injection procedure, as shown recently in CESR-c operation at low energy [22]. A second advantage, if the wigglers increase the synchrotron radiation integral I_3 more than I_2, is that the ring will have a larger natural energy spread, and therefore the value of I_{th} will be increased. On the other hand, a drawback introduced by the wigglers can be the effect of non-linearities on dynamic aperture and beam-beam behavior. Wigglers placed in regions with low dispersion and low beta values are less harmful.

The possibility of realizing a lattice with negative momentum compaction is included in the design. Negative α_c regimes correspond to shorter bunches, but lower I_{th}. [23]

The linear beam-beam tune shift neglecting crossing angle and hourglass effect is:

$$\xi_x = \frac{r_e}{2\pi\gamma} \frac{N}{\varepsilon_x}$$

$$\xi_y = \xi_x \sqrt{\frac{\beta_y^*}{\kappa\beta_x^*}}$$

(7)

The luminosity can be written in terms of the beam-beam tune shifts:

$$L_{bunch} = f_o \frac{\pi\gamma^2}{r_e^2} \xi_x \xi_y \frac{\varepsilon_x}{\beta_y^*}$$

(8)

The choice of emittance, horizontal and vertical β^* and coupling factor determines the beam-beam tune shift and the luminosity. We remark again the importance of maintaining the flexibility of choosing different sets of parameters in order to explore during collider operation the most effective regimes to increase the luminosity. Table III shows the tuning range of the most significant among them.

The approach to high currents is based on a careful design of all impedance creating elements in the ring, specially the RF cavity, and on the optimization of the feedback systems, as a natural evolution of the experience gained on DAΦNE. For the e- ring, ion trapping will be avoided by using small ICE made of Alumina coated with a thin layer of highly resistive material distributed along the ring, with a very small impedance contribution, and by filling the ring with a gap in the bunch train, while Ti coating and antechambers in the positron ring will fight the electron cloud instability.

The injection efficiency will be optimized by doubling the injection transfer lines in order to eliminate the time needed for switching between e+ and e- injection configurations.

The DANAE energy range goes from 0.5 to 1.2 GeV per ring. The maximum current at the maximum energy is limited to 0.5 A, in order to keep the total beam power within reasonable limits.

Injection is kept at low energy, so that the injection system does not need major modifications, and radiation shielding at injection is less demanding. Rings will be filled up to the operating current, and then ramped together up to the maximum energy.

Table III – Range of tunability of specific parameters for Φ operation. For each parameter the minimum and maximum values are given; the two columns do not represent a coherent set of parameters.

Parameter	Symbol	Units	Min	Max
Emittance	ε_x	mm mrad	0.2	0.5
Momentum compaction	α_c		-0.03	0.05
Horizontal β*	β_x^*	m	0.5	1.5
Vertical β*	β_y^*	mm	5	10
Coupling	κ	%	0.3	1
Half horizontal crossing angle	θ_{cross}	mrad	10	20
Number of particles per bunch	N	10^{10}	2.8	4
Bunch current	I_{bunch}	mA	13.8	20
Total current	I_{tot}	A	2	3
rf voltage	V	MV	0.4	1.5
Bunch length	σ_L	mm	8	15
beam-beam tune shift	$\xi_{x,y}^*$		0.025	0.06
Synchrotron tune	Q_s		0.02	0.10

Further upgrades

The basic DANAE design is based on already well assessed principles, on the present knowledge in collider physics, and especially on experience from DAΦNE. It includes however the possibility of adding new features, in order to open in the future other possibilities for increasing the luminosity.

One of these is the installation of **crab cavities**, which are beneficial to the beam-beam behavior, because they transform the collision with crossing angle into a head-on-like ones.

The long straight section opposite to the IR has available space for such a device, and the flexibility of the optics allows tuning the lattice for such a regime. Let's recall that the effectiveness of such devices will be tested in few months by the KEKB team on their B-factory, since in the present shutdown they are installing one crab cavity per ring [24].

Also the **Strong RF focusing** regime [15] could be implemented: the modulation of the bunch length allowing values of the vertical betatron function at the IP in the range of very few mm can be obtained by a regime with high RF voltage derivative and large dispersion in the dipoles, producing a drift of the longitudinal phase plane along the orbit. The regime in which the drift changes sign in the two arcs of the ring, corresponding to a small momentum compaction, can be applied to DANAE, with the high voltage cavity placed in a zone near the IR, in order to have the minimum bunch length at the IP. The necessary space for the harmonic cavity yielding the strong RF focusing is in fact foreseen in the ring layout.

COLLIDER DESIGN

Lattice design

The lattice of a Φ-factory based on a multibunch double ring with flat colliding beams is of course an evolution of the present DAΦNE design, with the modifications dictated by the past experience and the new available technology.

The ring layout consists of one IR, two arcs, the long and the short ones, and a long straight section opposite to the IR housing injection, RF and feedback systems. The two rings cross only at the Interaction Point (IP), while on the opposite point the two vacuum chambers are vertically separated avoiding parasitic crossings. In the central part of each arc there is a superconducting wiggler, to increase radiation and shorten damping times.

Emittance and momentum compaction can be tuned by varying dispersion and betatron functions in both arcs. The beams enter the IR from the long arc, and the section between the long arc and the IR is optimised to minimize the background induced inside the detector by particles scattered in the last dipole, while the rest of the background is shielded along the ring by a scraper system.

Figure 1 shows the layout of the rings inside the DAΦNE hall. The IR is centered in the same position as the present IR1 of DAΦNE, in order to reuse the existing KLOE detector infrastructures. Gray lines indicate the present DAΦNE rings, red and blue correspond to DANAE e$^+$ and e$^-$ rings and new transfer lines.

The Interaction Region (IR) design fits different energies and solenoid fields and is compatible with the KLOE detector.

The low-beta quadrupoles are based on the superconducting technology which is being developed for ILC [25], has been already successfully tested in HERA and CESRc and is being installed in BEPCII rings. The quadrupoles include skew and dipole coils, thus avoiding the mechanical rotation of quadrupoles and allowing closed orbit correction; the same technology provides the antisolenoid placed inside the detector [26]. Figure 2 shows a sketch of the IR layout.
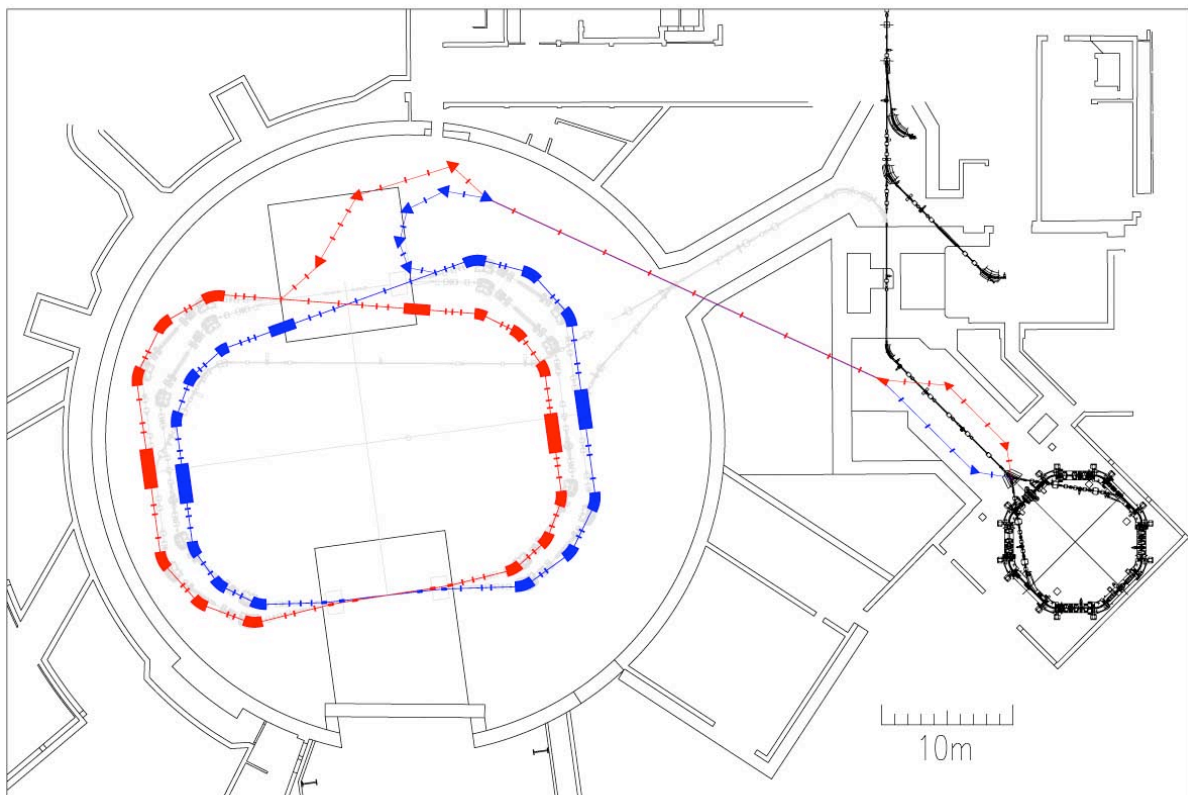

Figure 1 – Layout of DANAE inside the DAΦNE hall. Blue (red) lines correspond to e- (e+).

Figure 2 – Half Interaction Region schematic layout, showing quadrupole doublet and antisolenoid position.

Beams cross at a horizontal angle of 30 mrad providing the necessary separation at the first parasitic crossing for the Φ operation, where the distance between bunches is very small. The IR lattice is based on low-beta doublets, and the antisolenoid is placed just after the two quads, so that the coupling is corrected inside the detector. The vacuum chamber is common for the two beams in the detector zone, and splits just at the detector ends. Two downstream dipoles increase the separation between the beams. Figure 3 shows the horizontal and vertical trajectories in half IR for the Φ-energy, together with the beam stay clear, computed as $10\ \sigma_x,\ \sigma_y$.

Figure 3 – Horizontal beam separation and beam stay clear in m for E = 0.51 GeV.

Betatron and dispersion functions along the whole ring, for the two operating energies, are shown respectively in Figs. 4 and 5, starting from the Interaction Point (IP).
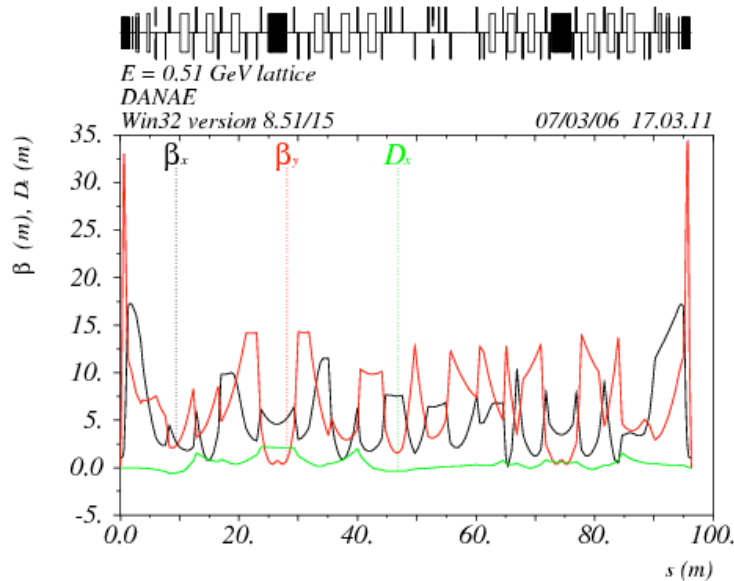
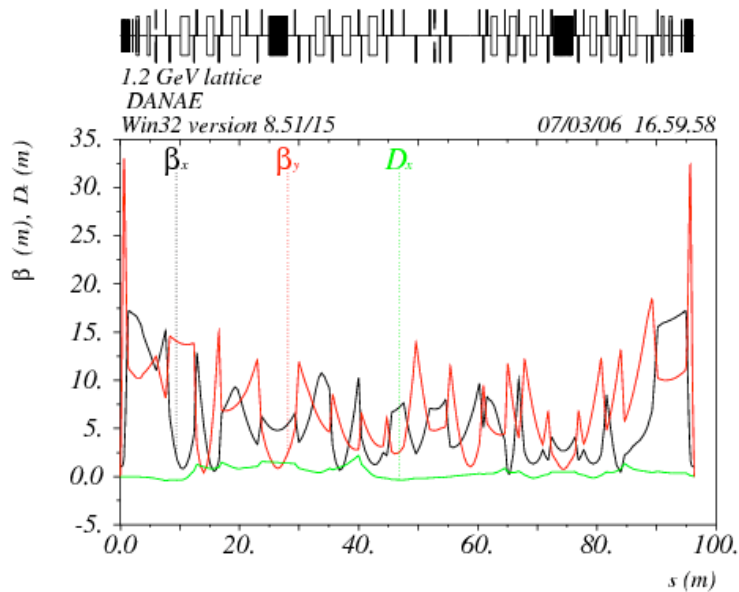

Figure 4 – DANAE Optical functions for the Φ-factory.

Figure 5 – DANAE optical functions for 1.2 GeV operation.

The dipoles are normal conducting ones, with a maximum field of 1.72 T at the maximum energy and 2.3 m bending radius. The dipole contribution to the damping is weak

$$I_{2\,dip} = \frac{2\pi}{\rho_{dip}} = 2.74 \, m^{-1}$$

and the presence of superconducting wigglers adds the necessary damping. In a wiggler the value of I_2 depends only on B_{max} and on the total length. Our nominal parameters

correspond to B_{max} = 4T for a total length of 6m per ring. The wigglers modify also the synchrotron integral I_3, which determines the natural energy spread and therefore the microwave instability threshold which depends quadratically on it. The choice of the pole length is led by the optimization of the nonlinear terms. For a given energy the trajectory oscillation amplitude depends quadratically on the pole length and linearly on the peak magnetic field. For a high magnetic field it is convenient to shorten the pole length in order to reduce the required transverse good field region, down to the value where the increase of the pseudo-octupole term, coming from the longitudinal drop of the field between poles becomes too harmful for the beam dynamics.

The values chosen for the design are summarized in Table IV. CESR-c wiggler design [22] has been followed for the choice of the number of poles: an even number of poles corresponds to a trajectory oscillating around the wiggler axis for any energy and/or any magnetic field value, and it is particularly convenient for a collider running under different operational conditions.

Figure 6 shows the magnetic field longitudinal distribution.

Table IV – SC wiggler characteristics

| Energy			0.51	1.2
Maximum magnetic field B_{max}	T		4	4
Total number of poles			19	19
Total length	m		2.96	2.96
Central pole length	cm		16	16
End poles length	cm		8	8
2nd and second-last poles length	cm		12	12
End poles field ratio to B_{max}			0.5	0.5
2nd and second-last field ratio to B_{max}			1	1
Max trajectory oscillation	mm		6	2.5
Path – wiggler length difference	mm		11.8	2.1
Total vertical beam stay clear	cm		2	2
Total horizontal beam stay clear	cm		8.5	8.5
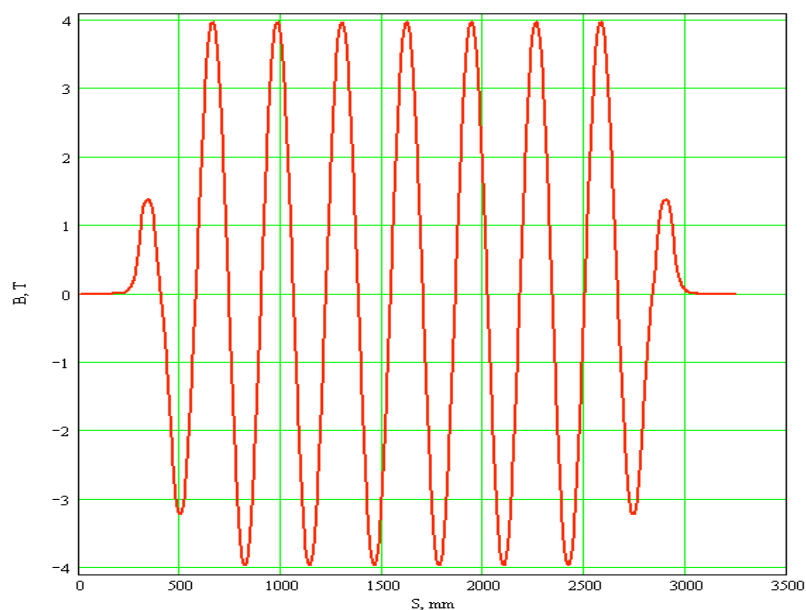
Figure 6 –Magnetic field distribution in the wiggler.

Beam dynamics simulations

The Φ-factory regime has been investigated more in detail and in the following the different beam dynamic simulations refer to the low energy case. All items are much less demanding for the case of high energy, and will not be mentioned in this paragraph.

Dynamic aperture

A large dynamic aperture is one of the essential characteristics of the Φ-factory both for the beam lifetime and the beam-beam behavior.

A first optimization of the dynamic aperture has been performed for the nominal lattice and the nominal tunes with no errors nor multipole components.

The sextupole configuration has been optimized by correcting to zero the natural chromaticity of the lattice. Table V shows the main parameters used for the tracking calculations and the results for the dynamic aperture in terms of the bunch sizes.

Table V – Parameters used in the tracking calculations and dynamic aperture results.

	Horizontal	Vertical
Betatron tunes	5.15	5.21
Natural chromaticity	-10	-19
Corrected chromaticity	0	0
DA on energy	25 σ_x	300 σ_y
DA off energy (0.5%)	17 σ_x	230 σ_y
DA off energy (1%)	9 σ_x	120 σ_y

Let's remark that the natural chromaticity is lower than the present DAΦNE one, even if the low beta value is smaller, since special care has been used in the linear design to minimize the chromaticity contributions in the whole ring.
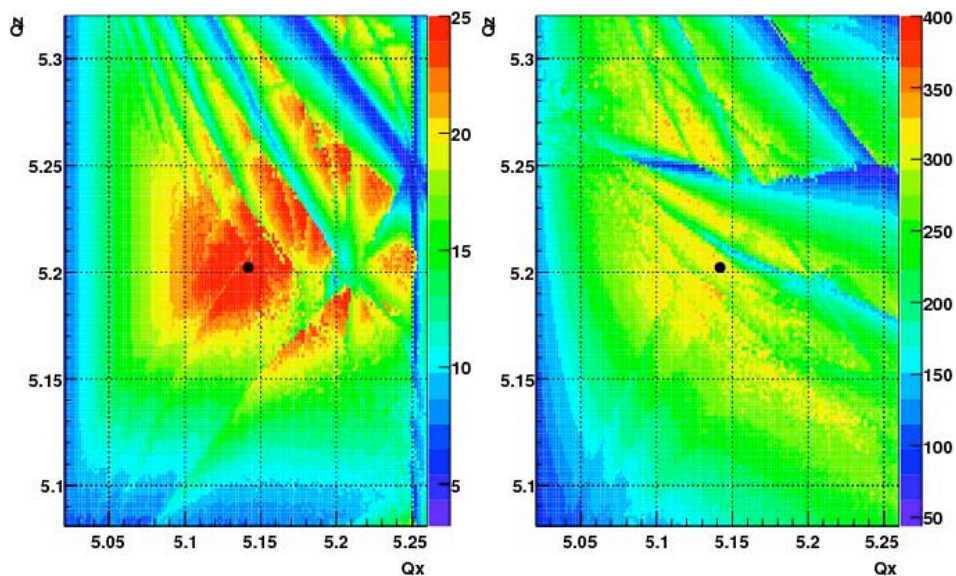

Figure 7 – Horizontal (left) and vertical (right) dynamic aperture betatron tune scans.

— 12 —

A total number of 15 sextupole families have been used The results are satisfactory: on energy the stable region is larger than 20 σ_x and 300 σ_y at the nominal coupling, and for the best configuration the off-energy dynamic aperture at 1% energy deviation (corresponding to 17 σ_p) is still 10 σ_x and 100 σ_y. With the best configuration a tune scan has been performed and the results are shown in Fig. 7.

Even if these results are already satisfactory, further optimization is foreseen in the future to explore the tune regions preferred by the beam-beam behavior, which stay closer to the integer, as shown in the next paragraph.

Beam-beam

In order to estimate the luminosity that can be obtained with the design parameters and to find the working points where the maximum luminosity can be achieved we have performed beam-beam simulations with the BBC code. The code simulates weak-strong beam-beam interaction in the 6D phase space including all principal effects influencing the luminosity: finite crossing angle, hourglass effect, longitudinal beam-beam kick etc.

The main parameters used in the simulations are listed in Table VI. Note that the bunch length at the nominal bunch current of 15 mA is 10 mm for positive momentum compaction (α_c=+0.02) and 8 mm for negative (α_c=-0.03), as given by the longitudinal dynamics modeling that takes into account bunch lengthening due to vacuum chamber wake fields.

Table VI – Beam parameters used for beam-beam simulations

Emittance	$\varepsilon_x = 0.45 \times 10^{-6}$ mm rad
Coupling	k = 0.3%
Horizontal beta	$\beta_x = 1.2$ m
Vertical beta	$\beta_y = 8$ mm
Energy spread	$\sigma_E/E = 5.4 \times 10^{-4}$
Number of particles	$N = 3 \times 10^{10}$
RF frequency	f = 500 MHz
RF voltage	V = 400 kV
Half crossing angle	$\phi = 15$ mrad
Momentum compaction	$\alpha_c = +0.02; -0.03$

In order to find suitable working points we have carried out luminosity scans in the tune diagram area Q_x = (0.05-0.15), Q_y = (0.05-0.15). We have chosen these tune intervals for our study since the area above the integer is well suited for low energy colliders like ADONE, VEPP-2M and DAΦNE. In particular, the maximum single bunch luminosity of 5×10^{30} cm^{-2}s^{-1} at the Φ-resonance was obtained by VEPP-2M at the tune ~ (0.06, 0.10) [27].

The tune scan (contour plot) performed for positive momentum compaction is shown in Fig. 8 on the left. The brighter red colors correspond to the higher luminosity while the green-yellow-brown ones indicate the strongest luminosity reduction (typically on beam-beam resonances). The maximum attainable peak luminosity is close to 10^{33} cm^{-2}s^{-1}, and is achieved at the tunes in the red area, near the point (0.06, 0.12). In turn, a luminosity around 9×10^{32} cm^{-2}s^{-1} can be obtained inside the magenta contours. Nevertheless the practical realization of these luminosity values is not simple since the safe tune area is small, the good working points are very close to the horizontal integer, where the dynamic aperture is intrinsically lower, and to the skew sextupole resonance $2Q_x = Q_y$ which can be dangerous both for the lifetime and for coupling correction.

The situation is much better if we exploit a lattice with negative momentum compaction (see Fig. 8 - right). In that case a luminosity of 1.2×10^{33} cm^{-2}s^{-1} can be obtained at the three working points: (0.06, 011), (0.05, 0.09) and (0.10, 0.06). Moreover, the tune area where luminosity above 10^{33} cm^{-2}s^{-1} is reachable is definitely much wider (see the violet contour areas).

Crab-cavities can improve the luminosity further (see Fig. 9). By comparing Figs. 8 and 9 one can see that the beam-beam resonances $2Q_x = Q_y$ induced by the finite crossing angle are eliminated in the crab-crossing scheme. The good "safe" areas become larger and, in principle, further luminosity increase is possible for higher (than design) bunch currents.
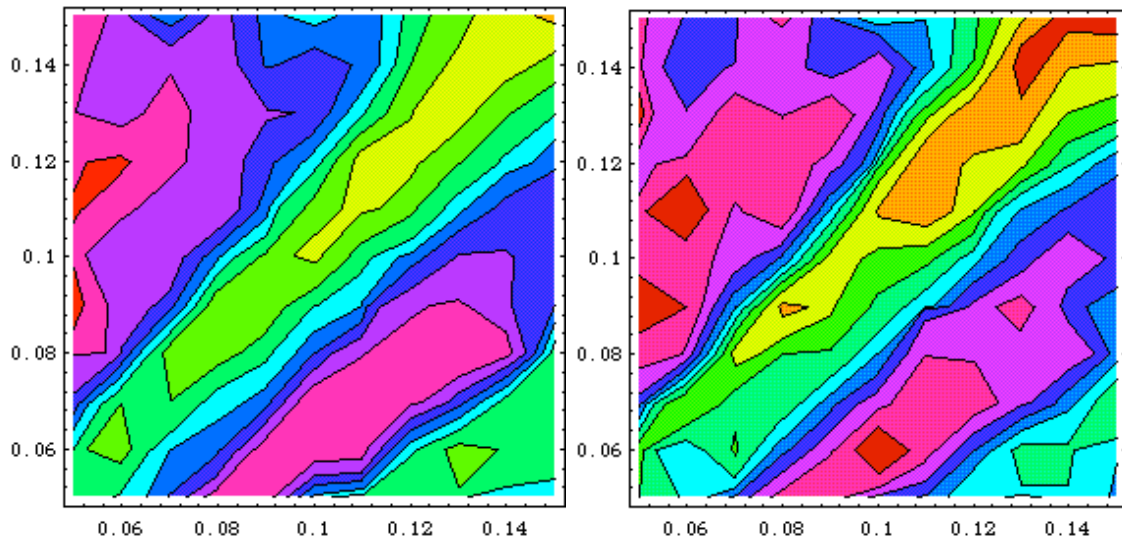

Figure 8 – Beam-beam simulations for positive and negative momentum compaction regimes at low energy.
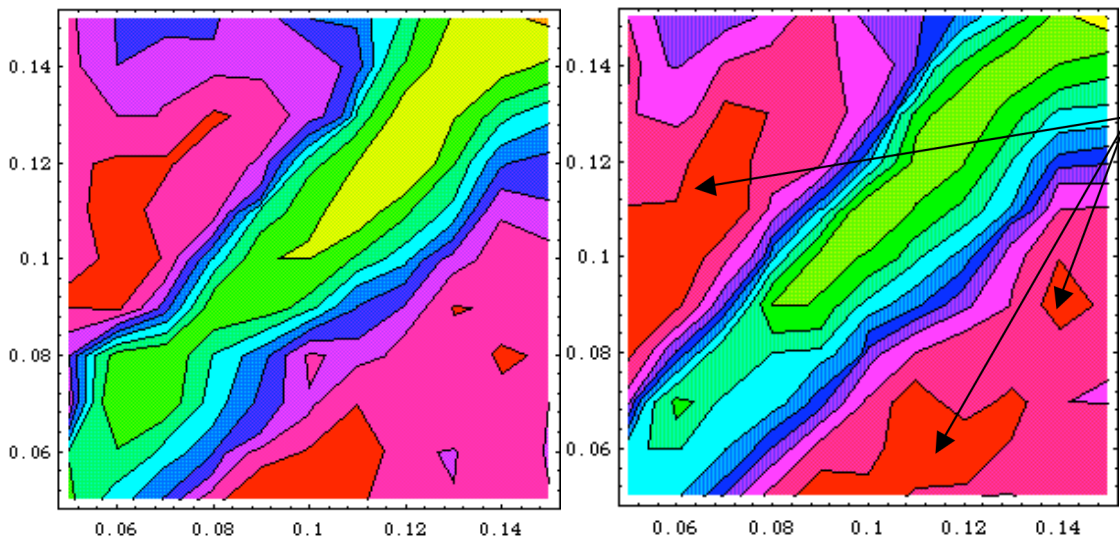

Figure 9 - Beam-beam simulations for positive and negative momentum compaction regimes at low energy with crab-crossing.

Bunch lengthening

In order to choose the parameters affecting the longitudinal dynamics a series of numerical simulations of the bunch lengthening in DANAE have been performed. They are based on the longitudinal wake fields calculated for the DAΦNE positron ring which proved to reproduce very well not only the bunch lengthening but also the internal motion in the positron ring bunches [28]. This is a reasonable, even conservative, approach since many DAΦNE vacuum chamber components will be reused in DANAE, and furthermore we expect to improve the DANAE beam coupling impedance with respect to that of DAΦNE.

The final results satisfying above requirements are presented in Figs. 10-14. In particular, as it can be seen in Fig. 10, with 400 KV RF voltage and positive momentum compaction ($\alpha_c = 0.02$) the bunch length at the design bunch current of 15 mA (3×10^{10} particles per bunch) is 10 mm (to be compared to 8-9 mm vertical beta function at the IP).

The threshold current for these parameters is higher than the design value. The threshold at about 20 mA is clearly seen in Fig. 11: it corresponds to the point where the bunch energy spread starts growing.
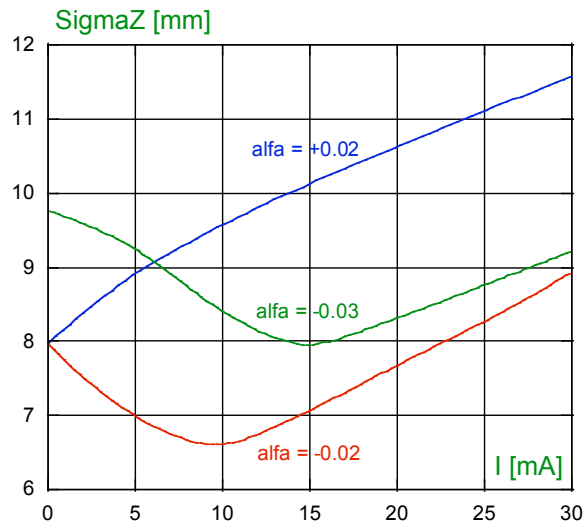

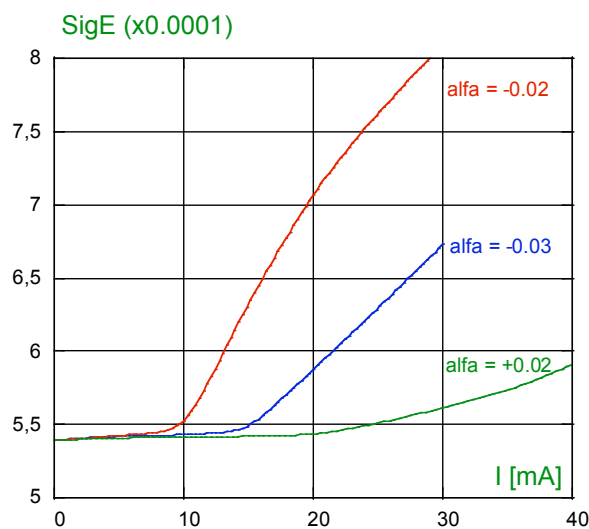Figure 10 - Bunch lengthening versus bunch current.

Figure 11 - Bunch energy spread versus bunch current.

Even shorter bunches can be obtained at the design current by using a lattice with negative momentum compaction. In this case the bunch shortens until the microwave instability threshold is reached. As one can see in Fig. 10 and Fig. 11, with $\alpha_c = -0.03$ the bunch at 15 mA is focused by the wake fields down to 8 mm without energy spread growth. It is also possible to obtain a shorter bunch length with a negative momentum compaction having lower absolute value. However, in such cases the design current becomes higher than the microwave instability threshold (see the plots for $\alpha_c = 0.02$, as an example).

The resulting bunch shapes for positive (+ 0.02) and negative (- 0.03) momentum compaction factors are shown in Fig. 12, while the corresponding bunch distribution centroid shifts with current are plotted in Fig. 13.
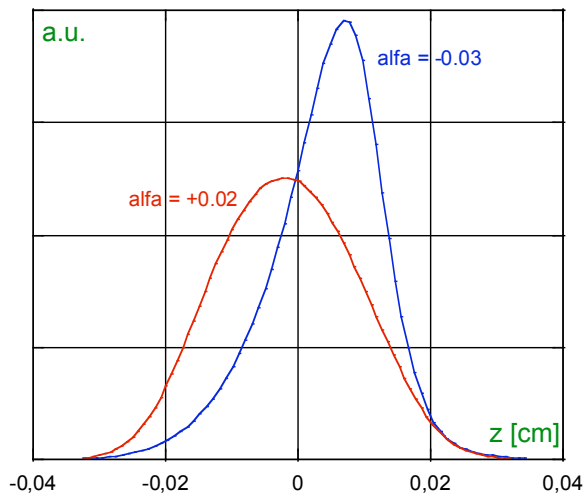

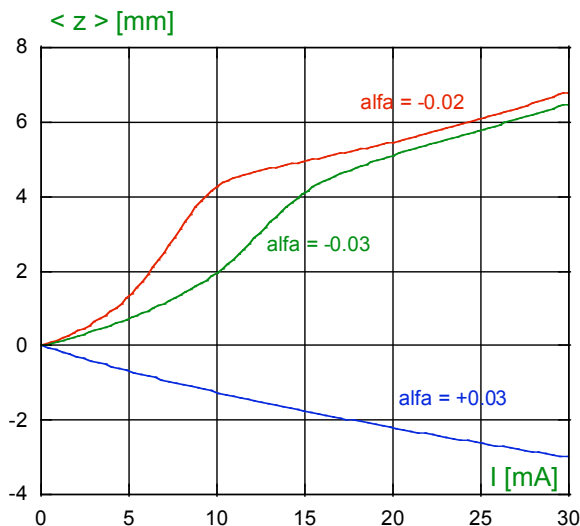Figure 12 – Bunch shape for positive (red) and negative (blue) momentum compaction factors.

Figure 13 – Bunch distribution centroid shift versus bunch current.

Touschek lifetime

The beam lifetime has been calculated taking into account the intrabeam scattering processes. With the aim to clarify the role of the localized betatron coupling correction over the IR, the calculation is performed with and without the IR contribution. Figure 14 shows BLT (Beam Life Time) vs. the emittance ratio at 10 mA bunch current for both cases. The difference is very small (few %).

BLT changes as the inverse of the bunch current at fixed coupling. Touschek contribution to the emittance and energy spread is negligible.

At the nominal current per bunch (15mA) and coupling (0.5%) the beam lifetime is of the order of 1000 sec.
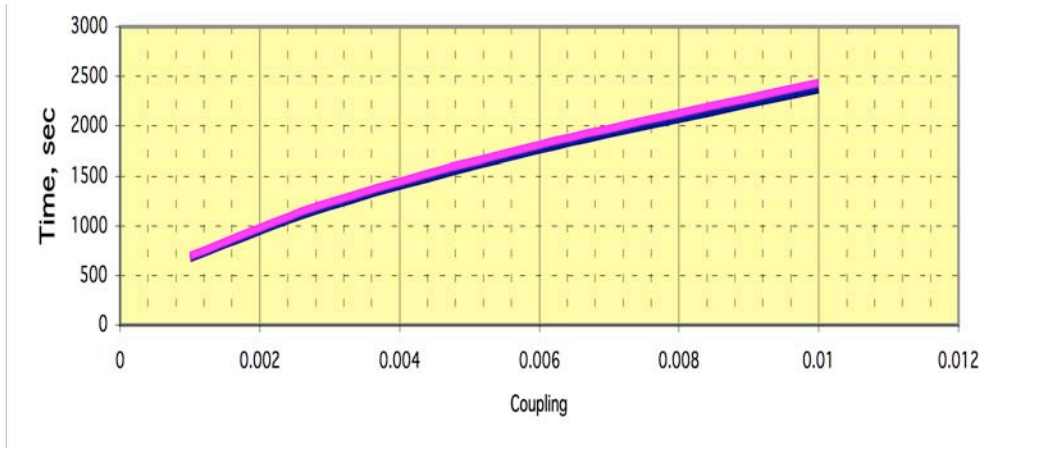

Figure 14 – Beam Life Time vs. emittance coupling at 10 mA bunch current.

Touschek background

Beam induced backgrounds will be dominated by Touschek scattering, as it is now for DAΦNE. Machine optics and vacuum chamber are designed to minimize losses as much as possible, especially at the Interaction Region (IR). Collimators are required upstream the Interaction Point (IP) to remove errant beam particles away from the detector. Shape and position of collimators must be optimized with simulations. Eventually, a masking system can be incorporated to shield the detector from beam-generated background. All these studies are performed with the same tools used successfully for DAΦNE [29].

Most losses arise from the Touschek scattered particles in dispersive regions, so only these particles are simulated. Touschek scattered particles have a betatron oscillation which is proportional to the dispersion D_x, to the invariant H ($\propto D_x$) and to the relative momentum deviation δp/p:

$$x = \frac{\delta p}{p}(|D_x| + \sqrt{H\beta}) .$$

The H-invariant parameter is defined by the following relation:

$$H = \gamma_x D_x^2 + 2\alpha_x D_x D_x^{'} + \beta_x D_x^{'2} .$$

The value of the *H* invariant (see Fig. 15) is for DANAE smaller by more than a factor two with respect to the one for DAΦNE, thanks to the fact that the emittance is created by a higher field in the wiggler. This reduces the betatron oscillations of the off-energy particles and, as a consequence, the overall particle losses around the beam pipe. However, since most losses are still at the IR, optics modifications are implemented to reduce this effect. Some examples of the scattered particles trajectories are shown in Fig. 16. They hit the vacuum chamber mainly at the focusing quadrupole QF downstream the IP; two scrapers placed about -8m and -12m upstream the IP can stop them.

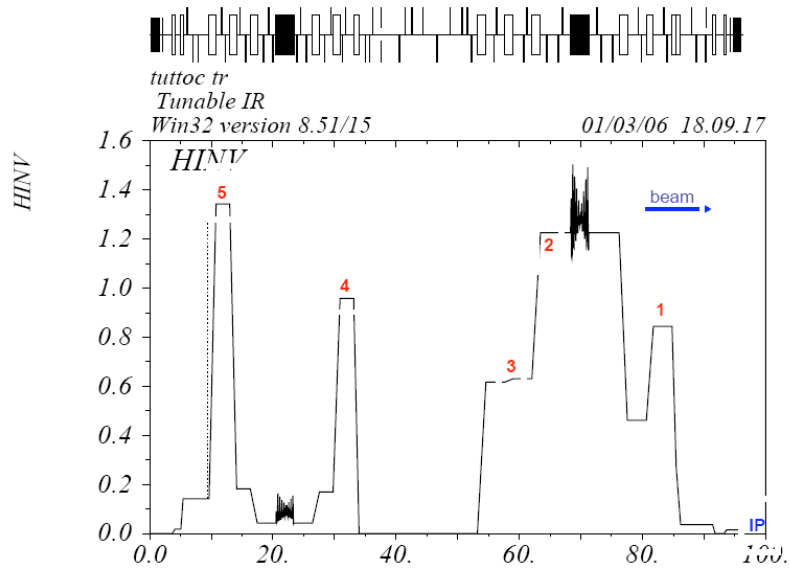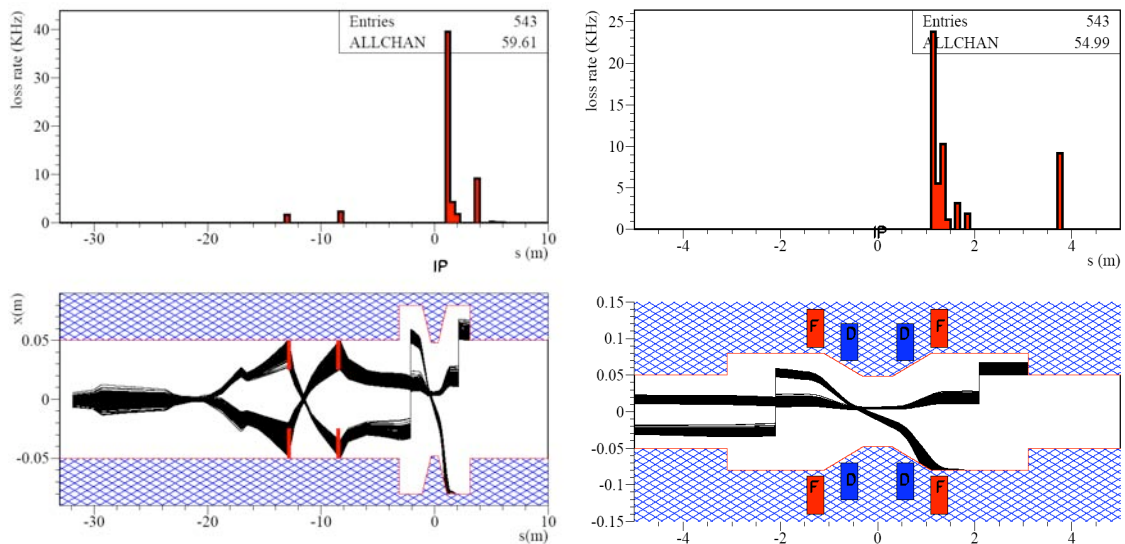Figure 15 – H-invariant along the ring. In red the regions where Touschek particles are generated.

Figure 16 – Trajectories (lower plot) and distribution (upper plot) of particles starting from region 2 upstream the IR and lost at the IR. Left plot is from region 2 to the IR, showing how two collimators can stop all particles which would be otherwise lost at the IR. Right plot shows the IR in more details.

COLLIDER MAIN SYSTEMS

A brief description of the main systems of the DANAE complex follows.

Magnets

Dipoles

The DANAE dipoles are dimensioned with a bending radius longer than the present DAΦNE one, so that the high energy can be reached with normal conducting technology and reasonable magnet gap (43 mm). With such a gap the best solution are the H shaped dipoles. A C shape solution with detachable poles would be very complicate from the mechanical point of view and, since the magnet must ramp up from 0.73 to 1.718 T, the connecting bolts between the various pieces of iron may represent a problem because of eddy currents. The required ramp up/down time must be further investigated, before freezing the magnet design. At this stage only a rough optimization of the magnetic field profile has been done by shimming the pole profile. More detailed 2D and 3D simulations are being accomplished to better evaluate the magnetic field profile. The main parameters of the dipole are listed in Table VII, Fig. 17 shows the Poisson simulation output. All the dipoles have the same bending radius, while there are three different magnetic lengths, as can be seen from the layout shown in Fig. 1.

Table VII – Dipole Magnet Parameter List

Energy	GeV	0.51	1.2
Nominal Field	Tesla	0.73	1.718
Bending Radius	m	2.329	2.329
Magnet gap	mm	43	43
Width	m	0.872	0.872
Height	m	0.683	0.683
Pole width at the gap	m	0.172	0.172
Pole width at the yoke	m	0.252	0.252
Nominal A*turn per pole	A	1650	33100
Turn per pole		64	64
Nominal Current	A	197,66	517.2
Current Density	A/mm^2	0.85	2.22
Copper Conductor	mm*mm	17.4*17.4	17.4*17.4
Cooling Hole Diameter	mm	9.3	9.3

The existing dipole or wiggler power supplies seem to fulfill well the required voltage and current values. However, since they have been designed for steady state operation, a set of measurements must be accomplished to verify the dynamic performances during the current ramp-up to determine if they can effectively be re-used for the upgraded machine. The different types of magnets will have different inductances, therefore only magnets of the same type can be series connected.
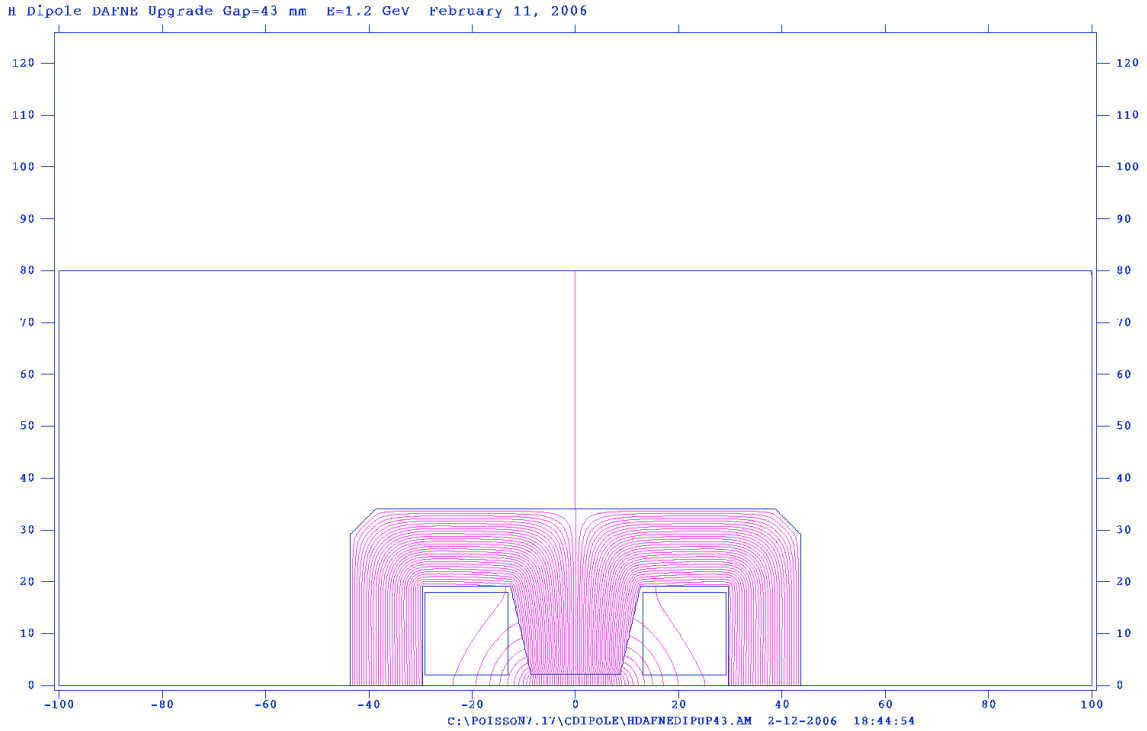
Figure 17 – 1.718 T Dipole Magnet, POISSON simulation output.

Quadrupoles and sextupoles

The total number of quadrupoles in each DANAE ring, not counting the IR magnets, is 46. The maximum integrated gradient is G_{max} = 4.5 T at the highest energy. Figure 18 shows the integrated quadrupole gradients for the two different DANAE regimes of the 46 quadrupoles in each ring.

The number of sextupoles used in the dynamic aperture computation is 15 per ring, but we intend to install some more to ensure flexibility in the future operation. The dynamic aperture has been computed up to now only for the Φ-factory regime, with a peak integrated sextupole gradient of 30 T/m in one family and much lower in all the others.

All DAΦNE quadrupoles, sextupoles, and correctors will be reused in DANAE. Table VIII summarizes the available quadrupoles and sextupoles of the DAΦNE rings with their main characteristics, which fit well the DANAE design.

Table VIII – DAΦNE available quadrupoles and sextupoles.

Type	Total number	Max integrated gradient	Magnetic length (m)
Large aperture quad	8	2.7 T	0.38
Large quad	28	2.7 T	0.29
Small quad	60	4.5 T	0.30
Large sextupole	18	26 T/m	0.15
Small sextupole	14	22 T/m	0.1
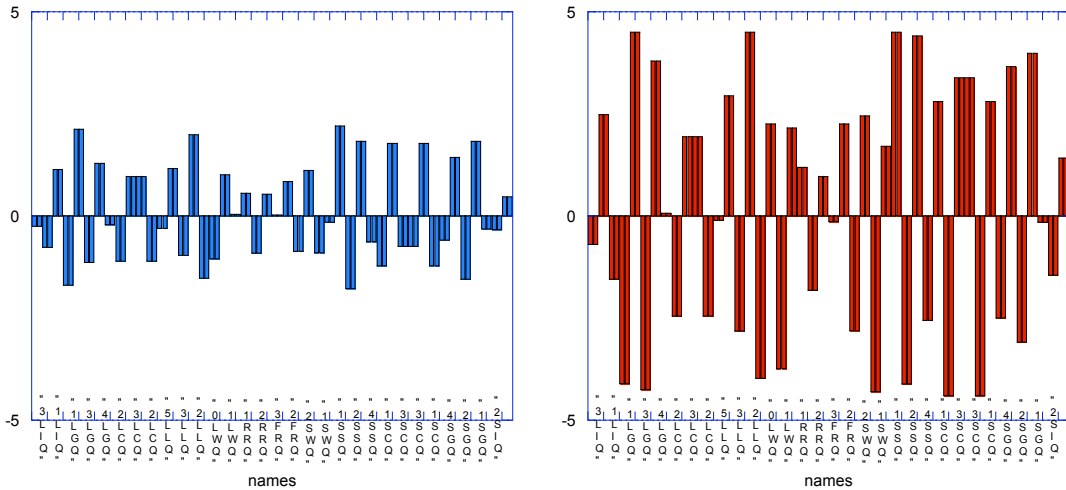
Figure 18 – Integrated gradient (T) for the Φ-factory (left plot) and the maximum energy operation (right plot) for the 46 quadrupoles in each ring.

Wigglers

Two wigglers per ring are used in DANAE for damping and emittance tuning. Their preliminary design, developed in BINP, is described here.

Wiggler magnetic system

The superconducting damping wiggler consists of 19 dipole bending magnets with field amplitude of 4 Tesla. Superconducting windings are made from Cu/Nb-Ti wires, which are placed inside a liquid helium vessel 4.2 °K during normal operation. A superconducting NbTi wire with lacquer insulation is used for the wiggler coils. The main parameters of the magnet are presented in Table IX.

Table IX – Wiggler main parameters

Maximum magnetic field B_{max}	T	4
Total number of poles		19
Number of main poles		15
Number of poles 3/4		2
Number of poles 1/4		2
Magnetic gap	mm	40
Number of turns at main poles		600
Current in coil	A	314
Total vertical beam stay clear	mm	20
Total horizontal beam stay clear	mm	85
Wire diameter with/without insulation	mm	0.91/0.85
Ratio of NbTi : Cu		0.43
Number of filaments		312
Critical current at 7 Tesla	A	380

The magnetic field in the wiggler median plane is created by 30 central and 8 side coils wound over the ARMCO-iron cores. The shape of the central pole is racetrack type. The coils of central poles are energized at 314 A.

The ARMCO-iron yoke is used to close the magnetic flux and to support the coils. The length of the magnet yoke is 3100 mm. The yoke includes two parts which are placed symmetrically above and below the median plane of the wiggler. The upper and the lower wiggler parts are supported by the non-magnetic stainless steel slabs located symmetrically between the halves. The additional iron plates between the upper and lower halves are used to close the stray magnetic flux. There are several technological facilities to orient and align the coils on the yoke. Special pins with rounded heads moulded into the cores of the coils are used for precision arrangement of all the coils along the longitudinal slot of the yoke. The bottom plane of the coil is in contact with the base plane of the wiggler bottom part. Thus, the horizontal alignment of coils is provided. The block of coils is pressed so that their orientation is perpendicular to the longitudinal axis of the wiggler. The dimension of the vertical magnetic gap between the coils is equal to 40 mm.

Cryostat

The magnet is placed into a special liquid helium cryostat (see Fig. 19) with a working volume of 330 liters liquid helium. The cryogenic system consists of an external housing, a 60 °K shield, a second 20 °K shield, a liquid helium vessel, a throat, a vacuum chamber with copper liner, an upper flange and a filling tube. The wiggler cryostat has four compact coolers used for cooling the shield screens and to prevent heat in-leaks into the helium vessel. During normal operation of the wiggler liquid helium consumption is close to zero. Liquid nitrogen is not used for cooling the shield screens.

Figure 19 – Overall view of the wiggler cryostat.

Two shield screens used to reduce the irradiation heat flux from outside surround the inner liquid helium vessel. The temperature on the outside shield screen is about 60 °K, on the inner 20 °K. There is vacuum insulation between the helium vessel and the 20 °K screen as well as between both screens and the 60 °K shield and an external warm stainless steel vessel to reduce the heat flux. The walls of the helium vessel face flanges with special stainless steel projections support the magnet. The vessel is hanged with four Kevlar strips connected to the external cryostat vessel. These strips pass through the external vessel walls and are used for precise alignment of the magnet. The wiggler vacuum chamber for the beam is a part of the liquid helium vessel and its temperature is 4.2 °K. To prevent liquid helium consumption due to beam heating a copper absorber is inserted into the vacuum chamber and is kept at 20 °K by two coolers.

Current lead block

Current leads blocks (see Fig. 20) are used to supply current to the magnet. These current leads are the main source of heat in-leak into the liquid helium vessel due to both heat conductivity and joule heat. Each current lead consists of two parts: a normal conducting brass cylinder and a high-temperature superconducting ceramics. One pair of current leads is assembled into one block together with a two stage cooler inside the insulating vacuum of the cryostat. The connection point between normal conducting and superconducting parts of the current leads is kept at 50-65 °K by a first stage of coolers. The lower part of the superconducting part of the current lead is connected with a superconducting Nb-Ti cable and kept below 4.2K by a second stage of the coolers. The power of the second stage is approximately twice more than the in-leak heat power at the lower end of the superconducting current leads and the rest of cooler power is used to cool the liquid helium vessel. This design allows obtaining an average liquid helium consumption less than 0.03 litres/hour and requires liquid helium refilling about once per year at normal operating conditions of the wiggler operation, together with routine maintenance of cooling devices.
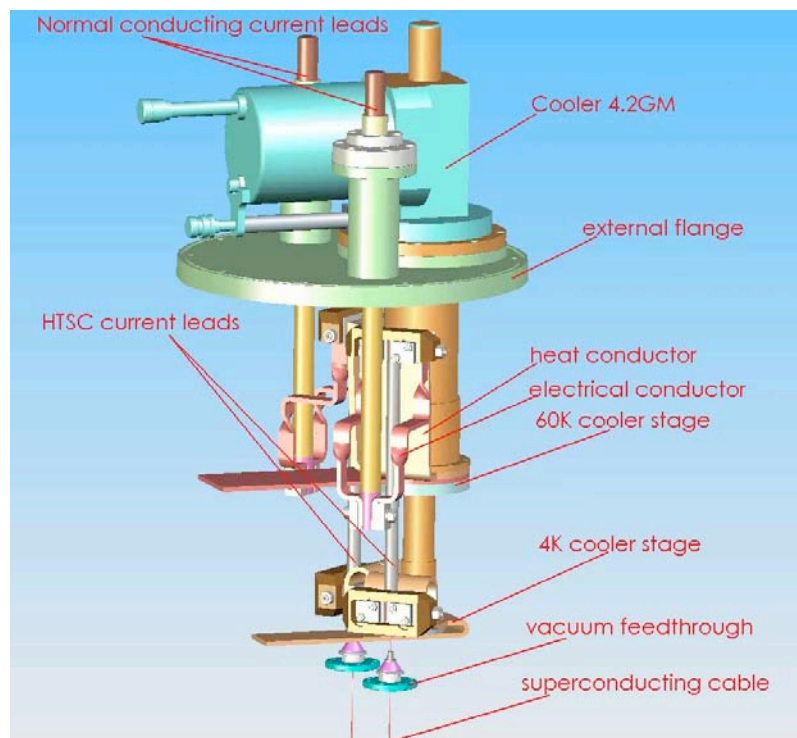

Figure 20 – Current leads block.

Low beta magnets

The low beta magnets inside the detector are based on the SC technology developed at BNL, already tested in different colliders, and proposed for the ILC final focus [13].

The main characteristics of the magnets are shown in Table X. The inner dimensions are determined by the beam stay clear in the presence of horizontal crossing, the outer ones by the available space inside the KLOE detector, and the requirement from the experiment of a 10° aperture cone free of machine components.

The maximum quadrupole gradients correspond to the high energy case, while the maximum longitudinal field of the antisolenoid is determined by the KLOE solenoid field at low energy ($B_z = 0.4$ T).

Table X – Low beta magnets design characteristics.

Magnet	QD	QF	Antisolenoid
Magnetic length (mm)	350	350	500
Inner radius (mm)	54 -> 71.5	82	82
Outer radius (mm)	71.5 -> 97.5	130	130
$G_{max}L$ (T)	11.2	5.6	
$G_{sk} L$ (T)	0.7	0.7	
$B_z L$ (T)			0.84

RF system

The DANAE RF system design is based on one single cell superconducting cavity per ring of the same type used for the KEK B-factory [30] (KEKB-SC cavity – see Fig. 21). The choice of a SC cavity is mainly motivated by the machine requirements for the high energy operation. An RF voltage up to 1.5 MV is required in this case, which cannot be obtained with a single cell copper cavity. The use of normal conducting RF technology would imply using more cells, bringing to a larger contribution to the machine broadband and resonant impedances, and requiring more RF power. At the present design stage we prefer to avoid this kind of drawbacks.

The KEKB SC cavities are in operation since 1999, and represent a mature and reliable technology. The cavity is basically a single cell structure with very large beam tubes to allow all the High Order Modes (HOMs) to propagate through, and being damped by ferrite loads placed on the beam pipe outside the cryogenic environment. The cavity loss factor is very small (k < 1 V/pC @ $\sigma_z = 8$ mm), so that the contribution to the machine broadband impedance is minimized, while all the HOMs result to be damped to a harmless level.

The input coupler is of coaxial type, and is routinely operated in KEKB at a power rate well above DANAE requirements.

The RF power required by the SC cavity to sustain the accelerating field is negligible, and the dimensioning of the RF source is essentially dictated by the amount of beam power to be restored. In the case of DANAE the beam power is maximum in the high energy operation, requiring an RF source capable of delivering up to 100 kW CW.

Klystrons rated for this power level at 500 MHz are available on the market, together with a variety of RF tubes used for TV broadcasting in the UHF band. An RF power source derived from a commercial broadcast transmitter is expected to be cheaper and more efficient. A market survey make a final choice is under way.
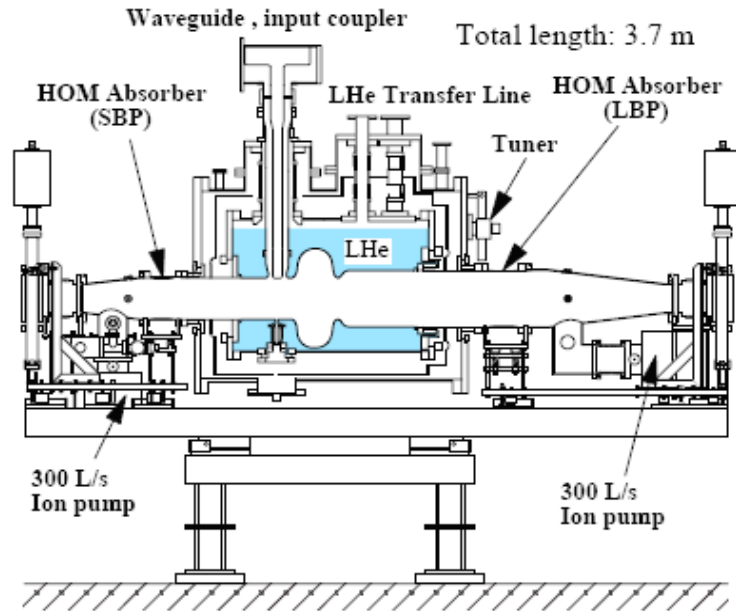
Figure 21 –KEKB SC cavity, very similar to the DANAE design.

Being the matching conditions between the RF power source and the cavity not guaranteed under all operating conditions, a high power circulator must be interposed to avoid damaging the RF tube.

A Low Level LRF (LLRF) control system has to be designed and implemented for the DANAE RF system because of the large beam loading expected. From the experience of the present generation factories, the interaction of the beam with the accelerating mode is the most delicate longitudinal dynamics issue. The techniques developed and used in these machines are fully adequate for DANAE.

In particular an efficient direct RF feedback system is needed to reduce the beam loading effects. Being the DANAE revolution frequency relatively high compared to that of longer machines, the accelerating mode is not expected to interact with revolution harmonics and sidebands different from the main RF ones. This simplifies considerably our LLRF design.

Standard RF servo loops, such as tuning, amplitude and phase loops are also foreseen.

Table XI summarizes the main RF parameters.

Table XI - RF system main parameters

		Φ-Energy	High Energy
RF frequency	f_{RF}	500 MHz	
max RF Voltage	V_{RF}	0.5 MV	1.5 MV
Cavity type		SC, KEKB-like	
Geometric factor	R/Q	46 Ω	
Quality factor	Q_0	$2 \cdot 10^9$ @ 4.2 K	
Cavity shunt impedance	R_s	92 GΩ	
Cryogenic RF losses	P_{RF}	1.5 W	12.5 W
Cryogenic static losses	P_{Static}	40 W	
Beam current	I_b	2.25 A	0.5 A
Radiation loss/turn	U_{rad}	21.4 keV	165 keV
Beam Power	P_{Beam}	48 kW	82.5 kW
RF source		100 kW CW, IOT or Klystron	
Optimal cavity-generator coupling	Q_{ext}	$32 \cdot 10^3$	$6.6 \cdot 10^3$

Feedback systems

The DANAE feedback systems are strictly related to the DAΦNE ones, of which they are the natural evolution. Let's consider the main upgrades for the best performance of the systems.

Longitudinal feedback systems

All the digital part of the systems currently used in DAΦNE need to be changed, while the analog front end and back end needs some modifications. The digital part, developed in collaboration with SLAC and LBNL in the 90's and based on a Digital Signal Processor (DSP) no more on the market, cannot work with the high synchrotron frequencies (up to 320 kHz) foreseen for DANAE. The limit of the present system is in fact <100 kHz.

A SLAC, KEK and LNF collaboration [31] is developing a new generation digital feedback design based on the Field Programmable Gate Array (FPGA) technology. More in detail, a prototype programmable bunch-by-bunch signal acquisition and processing channel with multiple applications in storage rings has been tested and operated in SPEAR-3, DAΦNE, PEP-II, KEKB, and the ATF damping ring. The processing channel can support up to 5120 bunches with bunch spacing down to 1.9 ns. The testing included applications as transverse and longitudinal coupled-bunch instability control, bunch-by-bunch luminosity monitoring and injection diagnostic.

The analog front end and back end must be adapted or changed to work with the new 500 MHz RF. In particular, a critical component is the comb filter, which is not commercially available, but the PEPII comb filter design can be reused for the DANAE feedback system. The power amplifiers can be used to feed the new longitudinal kickers.

Transverse feedback system

The four *transverse feedback system,* based in DAΦNE on an analog approach, can be upgraded with the same FPGA-based digital feedback. This upgrade will make easier to manage the betatron phase advance necessary to damp the instabilities, which now depends on the machine lattice. An FPGA-based prototype is currently running on DAΦNE to damp the e+ horizontal instabilities. A complete digital real time control of gain and timing with remote capability is also recommended to optimize the system overall efficiency. The analog front end and back end as well as the power section can be reused without big changes.

Feedback kickers

A *kicker for the longitudinal feedback* based on an innovative idea, a very wide bandwidth resonant cavity, was developed for DAΦNE [32] and the same type of kicker has been adopted worldwide in several feedback systems to damp longitudinal multi-bunch instabilities. The DANAE kicker design is based on the same principle.

The bandwidth of the working mode (TM_{010}) of the cavity kicker has to be $f_{RF}/2$, centered at $f_0=(n\pm1/4)f_{RF}$, where f_{RF} is the resonant frequency of the accelerating cavity and n is an integer: this because all possible coupled bunch modes are present in a frequency span between nf_{RF} and $(n+1/2)\,f_{RF}$ or between $(n-1/2)\,f_{RF}$ and nf_{RF}.

There are 2 main reasons for choosing $f_0=9/4 \; f_{RF}$. We have designed the cavity kicker for the Low Energy Ring of PEP-II[33], which is operating successfully. The DANAE f_{rf} (500MHz) is close to the PEP-II one (476MHz), and also the beam tube section of the two machines is almost the same. We can easily re-adjust the PEPII design to fit DANAE parameters.
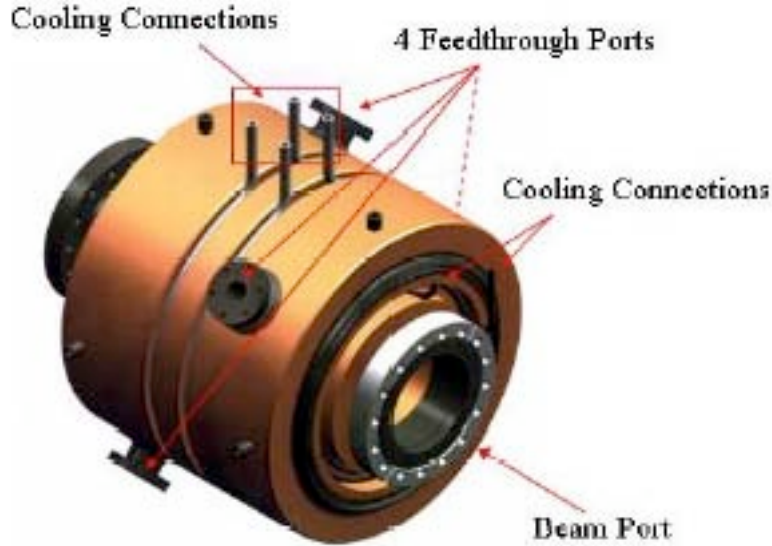

Figure 22 – PEP-II kicker for longitudinal feedback, designed by LNF.

The second important reason to prefer $f_0=9/4 \; f_{RF}$ is because in this case the working bandwidth is within the bandwidth of the solid state power amplifiers that are used for the DAΦNE feedback system.

Figure 22 shows the mechanical assembly of the PEP-II kicker. SLAC people decided to realize it in copper, but, being the kicker an intrinsically very low Q cavity, we think that it can be easily made of aluminum, as we have done for DAΦNE.

From a preliminary calculation, the sensitivity of the TM_{010} mode frequency to the cavity radius is $\Delta f/\Delta R=11.08$ MHz/mm. Therefore, to shift the frequency from 1.071GHz (PEP-II) to 1.125GHz (DANAE), the cavity radius should be reduced by something less than 5mm. Some adjustments are expected in the waveguide profile to avoid changing the bandwidth.

The *kicker for the transverse feedback* in DAΦNE has been realized as a strip-line electrode structure, and the same design will be used in DANAE. Two electrodes are placed on the opposite sides of the vacuum pipe and waves of the same amplitude and opposite polarity flow along them. There are two different devices, one to damp the oscillations in the horizontal plane and the other for the vertical ones. The shunt impedance, i.e. the efficiency of this kind of kicker, is given by:

$$R_s^{'} = 2Z_c \left(\frac{g_{trans}}{kh} \right)^2 \sin^2 (kl)$$

where k is the wave number, h is half the electrode distance and l is the electrode length. The values calculated with the shunt impedance of the DAΦNE kicker in the 0 ± 1GHz frequency range are plotted in Figure 23.
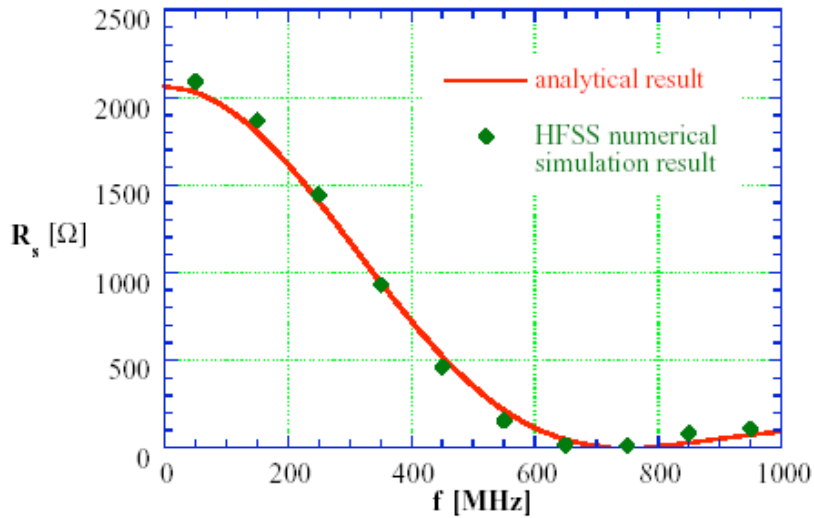
Figure 23 –Shunt impedance of the DAΦNE kicker.

For a given value of *h*, the longer is the strip-line the higher is the low frequency value of the shunt impedance, but long strip-lines have narrow bandwidth. As in the longitudinal case the coupled modes of oscillation are within a frequency range $f_{RF}/2$ wide. For DANAE this means having a sufficiently high response up to 250MHz.

To have high shunt impedance in the low frequency range and avoid strong drop at higher frequency, two kickers for each transverse plane can be used, one with a long strip-line and the other with a shorter one.

If the coverage angle of the electrodes is not too large both couples of strip-lines (for horizontal and vertical damping) can be placed in the same vacuum vessel, halving the number of devices required.

The strip-lines in the DAΦNE transverse kicker have a constant section. To lower the beam coupling impedance of the device, the strip-line can be tapered by reducing the coverage angle at their ends, as has been done for the new DAΦNE injection kicker design. In addition to a reduction of the broadband impedance, this solution allows to improve the frequency response of the transition between the strip-line and the feedthrough coaxial line. The uniformity of the deflecting field can be strongly improved as well. On the other side, for a fixed strip-line length, the efficiency is lower.

Diagnostics

The beam diagnostics play a crucial role for the achievement of the nominal performances. The diagnostic systems can be thought of as an evolution of those of DAΦNE.

We distinguish between different phases of operation, namely: a) commissioning, b) recovery after a major shutdown or an important hardware modification, c) machine studies, d) routine operation.

During phases a) and b) the beam charge is likely to be much smaller than the nominal one, and the beam behaviour is mostly dissimilar from what expected from a more or less precise machine model, for various reasons involving auxiliary systems, interlocks, computer control system etc.

Direct invasive diagnostics such as retractable (fluorescent) screens coupled with TV cameras can be tolerated and conventional laboratory instruments such as oscilloscopes and spectrum analyzers will be used to look at signals coming from various pick-ups. The absolute calibration and ultimate resolution of current and position measurement is not very important; on the other hand, the sensitivity to very small beam current, even in the presence of electrical noise, is considered most important.

Even not being a beam diagnostic system in a strict sense, a valuable complement to the conventional beam instrumentation in these phases can be given by suitable beam loss monitors distributed in various places of the facility.

During phases c) and d), most value of the diagnostic systems is assigned to precise absolute calibration of measurements and finer resolution of position, frequency (tune) and current measurement, for which a deeper integration in the computer control system is necessary.

We take the diagnostics presently operating in DAΦNE as a reference. Let's examine the requisites of DANAE. The increase of luminosity at low energy is based on the following distinctive features:

- -Shorter bunch length and lower β^* at the IP;
- -Stronger damping;
- -Higher number of bunches;
- -Higher colliding currents;
- -Continuous injection.

Each of the above features affects the diagnostics specification.

Shorter bunch length is well compatible with the streak camera presently used at DAΦNE.

Lower β^* at the IP implies, among other aspects, fine-tuning of the machine optics and tight control of the IP both in the transverse and longitudinal planes. The longitudinal control is well within the capabilities of the present RF and timing systems. The importance of having a more accurate working model cannot be overstressed.

The model is iteratively derived mainly from (difference) orbit and tune measurements. In first place the beam position monitor system must have the lowest absolute and relative accuracy, same for the tune monitor. The actual absolute and relative resolution (fractional mm and few tens microns, resp.) are probably adequate for DANAE, however, we suggest that single turn capability is added.

Single turn capability of the beam orbit measurement can considerably shorten the run-in during phases a) and b).

Turn by turn capability opens the possibility to measure directly the phase advance between monitors, to measure on-line the energy dispersion function and to apply modern analysis methods such as MIA [34] (Model Independent Analysis) for the refinement of the working model.

Tests of new electronic boards based on commercial units of characteristics adequate to DAΦNE are under way at DAΦNE.

Presently at DAΦNE we don't perform measurements of the incoherent *damping time*, which we deduce from the model optics. If a tighter control of incoherent damping is necessary, measurement can be carried out by looking at the decay of transverse beam size after a kick, using the present synchrotron light monitor laboratory.

The increase of *bunch frequency* is compatible with the existing diagnostic and feedback systems, provided that all resonant and/or tuned devices are re-adjusted according to the new RF frequency. For example, this implies the modification of the whole orbit measurement system anyhow.

Higher currents imply thorough comprehension of the beam transverse and longitudinal dynamics, reliable operation and margin of the feedback systems and RF servos. Moreover, the risk to exceed safe radiation levels and to damage the hardware of the accelerator and of the detector is bigger and uncontrolled beam losses must be prevented and avoided as much as possible.

We will pursue bunch-by-bunch capability in the measurement of charge, lifetime, transverse and longitudinal beam size, luminosity, transverse and longitudinal displacement and tunes. An all digital approach seems feasible using the fast G-Board [35] of the feedback systems. A relevant amount of software for time-domain and frequency-domain analysis has already been developed [36], and new software should be developed in such a way to guarantee compatibility and ease of use. The use of a fast-gated camera for transverse beam size and time gating in front of conventional laboratory instrumentation can be another successful approach.

Presently the (visible) synchrotron light from a bending magnet of DAΦNE is brought to an outside laboratory, accessible during operation. We plan to maintain this facility, with the addition of a beam line from a region with substantial value of the dispersion function to allow the observation of energy spread dependent beam size.

Although "button" pickups are at all suitable for the orbit system, we propose to employ 50-Ohm back-terminated stripline monitors as pickups for the feedback systems. Such devices with approximate length of <~ 15 cm can provide strong signal without reflections, which can be a possible cause of unwanted bunch to bunch coupling and must be minimized.

A beam loss monitor system similar to that used in DAΦNE, but with more sensors will be used in DANAE.

A beam abort system, based on a fast kicker must be provided to dump the beam in a controlled way at the occurrence of anomalies or beam misbehaviour. The kicker field must rise to a flat top in a time shorter than the ion-gap (presently ~ 8% of the machine length, or ~ 26 ns). In the beam abort line a spectrometer magnet can be added, allowing precise measurement of the incoherent energy spread.

The post mortem analysis can give important information, thus it is very important that all major accelerator systems provide adequate buffer memory of relevant waveforms, which can be stop-triggered by the abort trigger or by a sudden decrease of the stored current.

Continuous injection at high efficiency is necessary to keep the average luminosity high. For this scope, the injection process must be continuously monitored and corrected for possible drifts. The new transfer lines accommodate non-multiplexed single-pass BPM's after each bending magnet and quadrupole. Beam charge monitors of the thoroidal type (position insensitive) will be used along the transfer lines to localize beam losses and to initiate all the corrective actions.

Control System

Control System scheme

The Control System scheme focuses on a flexible integration of different elements.

All the devices must rely on a standard communication channel and the processors choice must not depend on constrains due to some *form factor*.

The DANAE Control System scheme adopts an Ethernet Gigabit switched network with many switches connected by fiber optic cables.

The present bandwidth of the networks (and its trend over the next future) makes them definitely suitable to sustain the whole control dataflow.

The Ethernet network is organized in different VLANs (Virtual Local Area Networks) in order to separate the various data flows depending on their nature.

This technique has been already adopted in the present DAΦNE Control System [37] and proved to be useful and reliable.

Processors

Concerning the processors, the Control System uses:

- a pool of servers for file system sharing, boot services, data storage, data sharing with the experiments, web access and service routines;
- many distributed diskless processors (of the order of 30-40) for the command and control of the machine devices;
- many consoles (of the order of 20) for the machine operators.

The general idea is to adopt as much as possible the same Operating System for all these processors. The recent experience with the DAΦNE 3rd level upgrade points out that Linux is a valid platform both for the servers and for the actual control of nearly all the machine subsystems.

Particular implementations will be faced with dedicated setups that will present their output over the Ethernet network.

Reuse of the DAΦNE Control System elements

The DAΦNE Control is strongly based on the VME bus *form factor*. Its main constraint is due to the fact that all the system dataflow is routed on VME-to-VME links. This means that all the processors dealing with the machine devices (as well as all the processors that must share data with them) must be VME embedded computers.

Redirecting all the dataflow from the VME-to-VME links to the Ethernet network, remove the above constraint. This will allow both to maintain the existing VME front end setups if they are still suitable and to introduce new ones (Compact PCI, standalone instruments, etc...) if an upgrade is needed.

Vacuum system

The DANAE vacuum system is aimed at generating the ultra low pressure needed to store the circulating beam and to reduce as much as possible the beam interaction with the residual gas inside the vacuum chamber.

Considering that DANAE is a variable energy and stored current machine, the vacuum system has to cope with both the worst operating conditions of high and low energy scenarios. The main parameters used to dimension the vacuum system, such as maximum currents and energy loss per turn, are those listed in Table II.

The DANAE vacuum system design is based on the assumption that the average operating pressure P is about 10^{-9} mbar and that the desorption coefficient η is about 10^{-6} molecules/photon.

Considering that the number of synchrotron radiation photons generated by dipoles is $9.3\cdot10^{20}$ photons s^{-1} for the low energy configuration and $4.8\cdot10^{20}$ photons s^{-1} for the high energy one, and that the number of synchrotron radiation photons generated by wigglers is $1.1\cdot10^{21}$ photons s^{-1} and $2.3\cdot10^{20}$ photons s^{-1} respectively, it is possible to estimate the total number of synchrotron radiation photons emitted. Through the desorption coefficient η, it is possible to estimate the total gas load Q and the needed pumping speed S.

The results are summarized in Table XII.

Table XII – Vacuum related parameters

		Units	DANAE @ Φ	DANAE 1.2 GeV
SR photons from bendings	$N_{\gamma b}$	s^{-1}	$9.3\cdot10^{20}$	$4.8\cdot10^{20}$
SR photons from wigglers	$N_{\gamma w}$	s^{-1}	$1.1\cdot10^{21}$	$2.3\cdot10^{20}$
Total SR photons	N_T	s^{-1}	$2\cdot10^{21}$	$7\cdot10^{20}$
Total desorbed molecules	N_{mol}	s^{-1}	$2\cdot10^{15}$	$7\cdot10^{14}$
Total gas load	Q	mbar l s^{-1}	$8\cdot10^{-5}$	$2.8\cdot10^{-5}$
Total pumping speed	S	l s^{-1}	80000	28000

The most critical case is the low energy configuration where a total pumping speed of about 80000 ls^{-1} is needed. For comparison, in DAΦNE 120000 ls^{-1} are installed. Anyway, the distribution of the gas load along the ring is probably different from that of DAΦNE, and so will be the arrangement of the vacuum pumps.

Synchrotron Radiation Power management.

In order to avoid vacuum chamber overheating, the synchrotron radiation power emitted by the beam must be dissipated. For this purpose a system of water cooled synchrotron radiation absorbers can be used. In this case the worst scenario is for the high energy configuration, where the total power emitted by the beam is $\approx$83 kW. This power is higher than the maximum value foreseen in DAΦNE, meaning that a new and more powerful system of synchrotron radiation absorbers must be carefully designed.

Vacuum Chamber Impedance.

In the DANAE vacuum chamber design it is mandatory to reduce the beam coupling impedance as much as possible in order to minimize bunch lengthening and longitudinal and transverse multibunch instabilities. The DANAE normalized impedance must be less than 0.5Ω in the spectrum range of the short bunch, i.e. vacuum chamber components must have impedance values smaller than the corresponding values for DAΦNE, which is one of the best machines from this point of view [38].

The pumping port and bellows RF shields must be improved using the innovative design introduced in the B-factory and developed by our group in the CLIC test facility ring [39]. Hidden slots design is foreseen for the pumping ports: long grooves along the vacuum chamber corners are created in order to decrease the impedance and inside the slots many holes prevent penetration of the RF field outside the beam pipe and guarantee the pumping

speed. The bellows are RF shielded by means of a continuous flexible contact that reproduces geometrically the inner of the rest of the vacuum chamber; the best contact configuration has to be studied depending on the vacuum chamber shape.

The vacuum chamber cross section remains constant as much as possible along the ring in order to avoid discontinuities and long tapers have to be used where different size chambers will be connected.

The high order modes that can resonate in the main cavities, in the injection kickers, in the longitudinal and transverse feedback kickers, and in all diagnostic tools must be suppressed. In the previous paragraphs the design criteria related to the impedance reduction of these components is described.

Ion Clearing Electrodes

In the electron ring the ionization of the residual gas due to interaction with the circulating electron beam is a well known phenomenon. The ions can be trapped in the beam potential well and move on stable oscillating orbits inside the beam. This *Ion Trapping* effect produces a general deterioration of the electron beam performances such as tune-shift, tune spread, emittance blow-up and enhancement of elastic and inelastic collisions with the residual gas. To reduce these effects three methods can be applied:

1. asymmetric filling pattern with a proper gap between stored bunches,
2. clearing electrodes located in the accumulations points,
3. transverse feedback to cope with the induced instabilities.

A clearing electrode is commonly made of an insulated alumina plate (thickness $\approx 0.6 \div 0.8$ mm), covered with a highly resistive paste ($R \approx 100 k\Omega$, thickness $\approx 0.2 \div 0.4$ mm), kept at a potential slightly higher than that induced by the beam.

During DAΦNE operation the electrode clearing system has properly worked [40], but with the drawback of the large contribution to the inductive impedance of the ring, due essentially to the 2 m long ICEs placed in the wiggler sections.

Calculations for different geometries and materials have been performed. The conclusion is that with a prototypal choice of a 64 x 44 mm alumina plate a total number of 30 electrodes with a relative dielectric constant $\varepsilon = 9$ and a thickness value $t_e = 0.3$ mm would give an overall contribution of about 0.06 Ω to the ring impedance, well acceptable in the impedance budget.

Injection system

LINAC

The LINAC [41] is on duty for the injection in the DAΦNE complex since fall 1996 and has accumulated about 60,000 hours of full performance operation.

Since 2001, in addition to the injection in the storage rings, the LINAC is utilized to provide electron beams to the Beam-Test Facility (BTF). BTF operation can be carried out in parasitic mode during DAΦNE operation.

Therefore the LINAC is being used since almost a decade; also, due to the stringent requirements of the operation of a Φ-factory, regular and frequent maintenance is somewhat difficult to plan.

The DANAE project does not require upgrading the present LINAC parameters, which are briefly listed in Table XIII.

Table XIII - Main Linac parameters

	electron	positron
Max output energy (MeV)	800	550
RF frequency (MHz)	2856	
Number of klystrons	4	
Klystron power (MW)	45	
Number of HV pulsed modulators	4	
Number of accelerating sections	15	
Max repetition rate (Hz)	50	
Beam pulse width (nsec)	$1 \div 10$	
Output beam current (mA)	300	80
Output emittance (mm.mrad)	< 1	< 5

On the other hand, due to the long period of operation and to further activity foreseen to complete the DAΦNE experimental program, few LINAC key-components need to be renewed or replaced.

The most stressed components of the machine are the klystron HV power modulators. They have been operating since their initial full power tests at the factory site in 1994. Their design concept goes back to the late 80's and some spare parts are not available so far or difficult to find. The use of modulators of modern design is therefore recommended to face a new long period of operational activity.

The LINAC is at present controlled through a CAMAC system which is not compatible with the storage rings VME system. It will be replaced with a new one so to be fully integrated with the new DANAE control system.

The positron converter system requires few improvements as well. The focusing coil power supply will be reviewed and possibly replaced with a more reliable system.

Other systems such as the waveguide network and the accelerating sections have operated satisfactorily and do not require modifications or special improvements.
The vacuum system will be also updated with a new pumping system.

New injection transfer lines

DANAE needs a very efficient injection system to store in the collider very large average currents in very short time. To keep a good average-to-peak luminosity ratio, high efficiency injection is mandatory due to the short beam lifetime dominated by the Touschek effect, enhanced by the small longitudinal and transverse bunch sizes, and by the beam-beam bremsstrahlung. For this reason we propose an improvement of the present injection system, with the aim of realizing a flexible structure capable of running under different operating conditions, ranging from a limited duty cycle, compatible, for example, with the requirements of the Synchrotron Radiation and BTF facilities, to continuous injection in the low energy configuration to keep the average and peak luminosity very close.

The present powerful injection system, composed by a full energy electron and positron LINAC and an accumulator-damping ring, will be reused after some minor modifications necessary to fulfill the efficiency and reliability requirements.

The operational stored current in the DANAE electron and positron main rings is $\approx$2.5 A/beam in 150 bunches, corresponding to 3.2×10^{10} particles per bunch. We assume to refill 1/3 of the bunch current in the main ring at each injection shot. If the transport and injection efficiency from the Accumulator and main ring is close to 100%, the current stored in a single bunch of the Accumulator must be, scaling the main ring length with the Accumulator one, 15 mA: this value is routinely achieved in the present configuration.

In the actual configuration the time needed to switch the LINAC and the transfer lines from the electron to positron mode of operation is longer than the refill time of each bunch. The most time consuming operations in the switch are the transfer line magnet polarity change and set up, the positron converter insertion, the solenoidal field set up for the positron capture section , and switch on of LINAC chicane.

New separate transfer lines, one for the electron and one for the positron beam, between the Damping Ring and the Main Rings are proposed in order to avoid the magnet polarity switch from electron to positron mode. Not only the main rings refill is more efficient but also the reliability of the injection process will be improved because no active elements but two pulsed magnet are changed.

The transfer line from the LINAC to the accumulator remains in common and this line has only one pulsed element that switches polarity between electron and positron transport; the time between two polarity switches is of the order of 100 ms, equivalent to 5 damping times in the damping ring. The layout of these new transfer lines is shown in Fig. 1.

With this scheme continuous injection in the main ring is possible with a repetition rate up to 5 Hz. The option to refill all the positron bunches and then all the electron ones is also valid without any hardware change respect to this scheme.

Reuse of all the dipole and quadrupole magnets of the present transfer lines, power supplies and diagnostic devices is foreseen.

Injection kickers

New kickers have been designed for the injection upgrade in DAΦNE and as injection/extraction devices for the International Linear Collider (ILC) damping rings [42]. The same kickers will be used for DANAE.

The design is based on a new idea to taper the striplines in order to reduce the impedance of the device and to improve the deflecting field quality at the same time. They have short pulse ($\approx$5ns), very good uniformity of the deflecting field, low broadband impedance and repetition rate up to 50 Hz.

The short pulse perturbs only the injected bunch and the two adjacent ones, strongly reducing the perturbation of the stored beam. The expected improvements are first of all the possibility of storing higher currents in the positron ring, since at present the current threshold is related to the excitation of transverse instabilities at high currents under strong perturbations at injection; secondly, the background in the experimental detector will be reduced during injection.

The structure is fed by high voltage (50 kV) short duration (5ns) pulsers. The first high voltage tests on the feedthrough are now under way and the kickers should be installed in DAΦNE in one of the next shutdowns. The mechanical drawing of the device is shown in Fig. 24.

Figure 24 - DANAE kickers

Timing

The present DAΦNE timing system can manage harmonic numbers up to 256 and it is able to work with a clock >500MHz, so in principle the system can be reused without any changes. Nevertheless, the following points can be discussed for the new machine.

If the new injection system will need more status bits in the timing command word for the presence of new injection devices a more powerful approach will be necessary.

From a technological point of view the DAΦNE timing system is based on 100ECLinPS parts that are still a very good component family and on the no more available ATT1610 digital signal processor. An upgrade of the DSP modules could be considered but, in this case, a simple porting of the firmware will not be possible and the hardware must be completely redesigned.

Ramping

Mantaining the injection energy at ≈ 510 MeV requires that a ramping procedure must be implemented in order to reach the high energy regime.

The main issue in an energy ramping process is to change the accelerator energy in a time as short as possible without beam losses. Keeping the ring optics fixed during ramping is the best way to avoid crossing harmful resonances, instabilities and beam losses due to large orbit distortions.

In principle the energy ramping procedure can be implemented in three simple steps:
- separation of the two beams at the IP.
- synchronous ramping of both rings from injection energy to the desired interaction one.
- removal of beam separation.

Beam separation can be realized in the longitudinal plane by a fast phase jump of the RF cavity in one ring or in the vertical plane by a closed orbit bump.

The ramping process involves all magnetic elements except the SC wigglers and the detector solenoid: a correction procedure for scaling the optics will be implemented, to compensate for the effects of such devices which do not scale with the energy. To be mentioned that non –exact compensation of the solenoid at low energy is beneficial since it increases the beam lifetime. Dedicated High Level Software (HLS) applications, running within the collider Control System, will be used to control all power supplies which have a remotely settable slow-rate and accept an external hardware trigger. Figure 25 shows a sketch of the system.

All magnetic elements are of the laminated yoke type, but the thickness of the vacuum chamber must be also taken into account. For example the DAΦNE vacuum chamber is compatible with a ramp time of the order of 40sec, and the vacuum chamber of DANAE has to be designed in order to allow a reasonably fast ramping speed.

In order to estimate the time necessary to inject from scratch 0.5 A in each beam and reach the colliding condition, we take into account the calibration of the DAΦNE elements:

- 30 steps are a reasonable choice to make the different calibration curves compatible and $t_{\text{ramp}} \approx 2$ s is a conservative assumption for changing the currents from power supplies.
- at each step 2 s are required for the slow orbit and betatron tunes feedbacks, which are implemented to correct residual distortions of the ring optics
- 90 s are needed to inject 0.5 A in both beams.

The typical operation will be:

- ramp down from operation to injection energy: 120 s (2 s for the magnets + 2 s for the slow feedback at each step)
- injection of the beams: 90 s
- ramp up to operation energy: 120 s

The total time is ≈ 7 minutes. This time is quite reasonable if compared with the estimated beam lifetime in collision, of the order of 2 h.
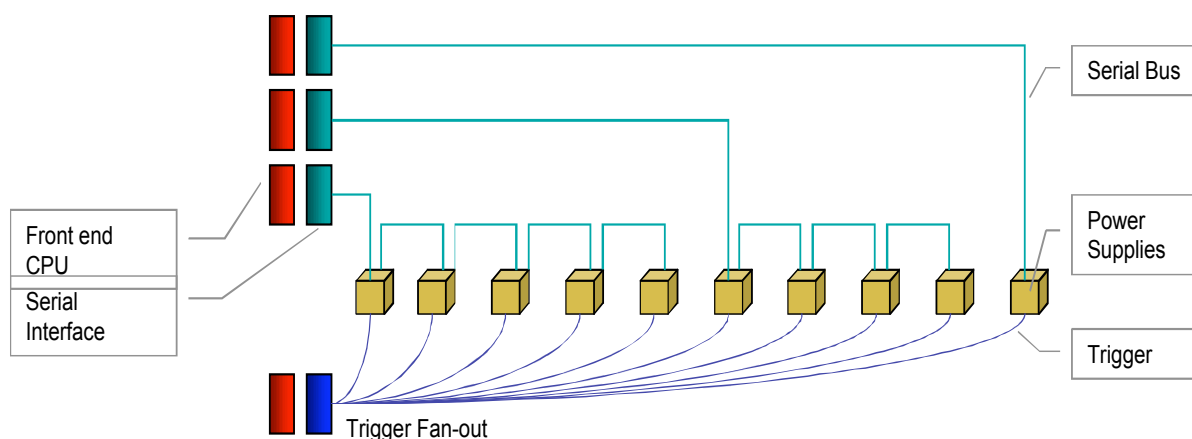

Figure 25: Power Supply synchronization scheme.

Cryogenic system

For the DANAE cryogenic loads the performances of the present LINDE TCF-50 cryogenic plant of DAΦNE must be investigated, in order to evaluate possible upgrades.

The present configuration of the plant accounts for the following nominal loads of the DAΦNE accelerator SC magnets:

100 W @ 4.4 K
800 W @ 70 K
1.4 g/s LHe

used for the supply of KLOE and FINUDA solenoids and the compensator magnets. The nominal cryogenic power of the TCF-50 with KAESER 440 compressor, as stated by the manufacturer is 300 W @ 4.4 K.

In the DANAE project the cryogenic load will be:

1. KLOE solenoid
2. 4 SC wigglers
3. 2 SC RF cavities
4. 2 IR SC sections

The SC wiggler is being designed in BINP. They can cool the wigglers by compact cryocoolers by Leybold and SUMITOMO HI. Each wiggler uses two 2-stage coolers for shields cooling and for interception of heat from current leads (Leybold Coolpower 10MD or Sumitomo 10K Closed Cycle Refrigerator system SRDK-408S-W71D). In this case liquid helium consumption is less than 1 litre/hour. To provide zero liquid helium consumption each wiggler can use additional two 2-stage coolers (Leybold 4.2 One Watt system or Sumitomo 4K Closed Cycle Refrigerator system SRDKD2-W71D). So the wigglers can be considered as a stand alone cryogenic system.

A very preliminary analysis of the 2 SC RF cavities led to of a static load of 150 W @4.4 K for the whole system.

About the IR SC sections no thermal analysis has been performed yet. Cooling the sections with dedicated cryocoolers system as well is the preferred option, but it must be investigated in detail.

At this stage it is difficult to say if no major modification of the present DAΦNE He refrigeration plant will be necessary. To increase the power of the plant means to change the He compressor motor size and to restyle the Cold box Heat exchangers, which is expensive and time consuming.

If the IR SC section can also be a stand alone cryogenic system, probably only a revision of the distribution system (valve box and transfer lines) will be necessary.

A more detailed analysis and definition of the loads is under way.

Cooling system

The design of cooling system aims at re-using most of the existing DAΦNE facilities, although undertaking a restyling due to different requirements, enhancing the reliability and the availability of the whole system coming from a lower global power dissipation load, mainly due to the adoption of cryogenic wiggler magnets.

The main actions will be:

- The three subsystems of the DAΦNE water cooling plant (LINAC, Transfer Line and Damping Ring, Main Rings) will be unified, thus minimizing the number of major points of failure and maintenance, such as cooling towers, heat exchangers, pumps, etc. As a consequence, some of the components now installed in access restricted areas will be dismissed or moved, to increase the effectiveness of maintenance and operation.
- The piping networks will be integrated, with minor local changes.
- Most machinery will undergo cures due to ageing; some of them will be replaced.
- The control devices will be adapted to meet DANAE requirements.
- The facilities for the treatment of water (demineralized and tower water) will be upgraded.
- Some of the air conditioning small independent plants, supplying some subsystem, will be centralized and upgraded to the new operating conditions.
- Consequently to all the changes, the supervisory system will be updated.
- Finally, a period of commissioning has been scheduled.

Care will be paid to revise the new requirements, owing to the fact that original design of the DAΦNE water cooling system adopted relatively high temperature levels (32°C inlet), to permit the use of cooling towers instead of more expensive and less reliable chillers.

Power Supplies

In the DAΦNE complex there are more than 500 power supplies. Most of them will be reused for DANAE, with the necessary maintenance which includes in some cases substitution of opto-couplers, power switches, power filter capacitors and cooling elements, according to the different types of devices.

Observation during DAΦNE operation has given during last year a MTBF (Mean Time Between Failure) for the power supplies of:

MTBF= (60 days*24 hours/day)* (500 power supplies)/ (Number of Faults in 60 days)

$MTBF_{2005}$=60*24*500/10=74000 h

A preliminary analysis of the possible choice of power supplies typology for the new DANAE dipoles has shown that the present wigglers end poles power supplies can be used for the three different dipoles families.

We remark that the power supply performance during ramp must be validated to check for uniform behavior of all power supplies and the tuning of control electronics must be obviously updated and tuned to meet the new load characteristics.

Electric installation /power supply

DAΦNE, at the moment, is powered by 4 medium voltage substations with a total LV transforming capability of 20 MVA.

- Comparing main electrical loads at the present status of DANAE design with the DAΦNE ones, we can remark that LINAC, Transfer Lines and Damping Ring are equivalent.

- Main Ring Dipoles load is expected to be a bit larger, but the magnets of each ring should be connected in three different families. As a result we will use six low voltage power supplies instead of one MV.
- 4 superconducting wigglers will replace the present 8 normal conducting one (-2.5 MW).
- Quadrupoles load will be more or less the same;
- Normal conducting RF cavities will be replaced by SC ones (-0.5 MW);
- Only two splitters (not yet estimated) are necessary instead of four;
- The cryogenic system will be integrated by local cryocoolers or powered in order to supply SC wigglers; SC RF cavities cooling is under study and may require a relevant increase in power request.
- Due to reduced thermal load, the water cooling system electrical load will be smaller.

Cyclic energy ramping has to be evaluated in order to estimate voltage fluctuations and flicker effect. Rise and fall time and repetition rate in the operation are relevant parameters in order evaluate this problem. At a first glance, with a repetition rate of tens of minutes and the expected load, this should not create a problem.

As a conclusion, no relevant electric installations are to be taken into account.

DANAE FACILITIES

BTF

The compatibility with DANAE of the Beam Test Facility of Frascati (BTF) is evaluated, in order to investigate the possibility of operating it successfully as in the case of DAΦNE.

The main purpose of the facility [43] is to provide single electrons or positrons for detector calibration and low energy electromagnetic interaction study. These particles are obtained by attenuating the high current LINAC beam (a typical spill contains 10^7-10^{10} electrons/positrons) by means of a tunable thickness target where the beam is degraded. An energy selection system, downstream the beam degrader, composed by a calibrated magnet and collimators allows selecting single electrons/positrons with an energy resolution of 1%.

Figure 26 shows the BTF experimental hall, ≈100 m^2 fully equipped for users with permanent DAQ, gas system, remotely controlled table, racks, crates, crane, high and low voltage power supplies and electronic pool.

Figure 26 - The Beam Test Facility experimental hall.

As already described in the injection system paragraph, few mA of stored current per pulse are needed to continuously top up the DANAE main rings. Typically no more than 20 Linac pulses, with an average current of 30 mA, have to be accumulated in the damping ring before extraction, transport and injection in DANAE. This means that at last 30 pulses out of 50 available from our Linac can be used for other purposes, such as the test beam. A fast electromagnetic pulsed magnet (with a rise time of 15 msec) can be used in order to extract the beam from the transfer line to the test beam area, allowing simultaneous operation of DANAE and BTF. The number of pulses transported to the BTF area can be optimally modulated by varying the duration of the pulse from DC operation (50 pulses to BTF) down to a minimum of a single shot. One pulse can be anyway sent to the hodoscope system for energy measurement and injection tune up.

In order to operate the BTF in the new injection scheme proposed, a LINAC current feedback is needed to keep constant the flux of particles in the BTF area (see Fig. 27).

Two systems are under study:

- Slow collimators feedback based on a high sensitivity Beam Current Monitor (BCM), with a typical time needed to operate of order of seconds.

- LINAC pulse modulation, in which the LINAC current can be modulated by adjusting the pulse to the gun cathode shot by shot. This second scheme is much more interesting because it can minimize the beam loss, and decrease the background in the experimental area.
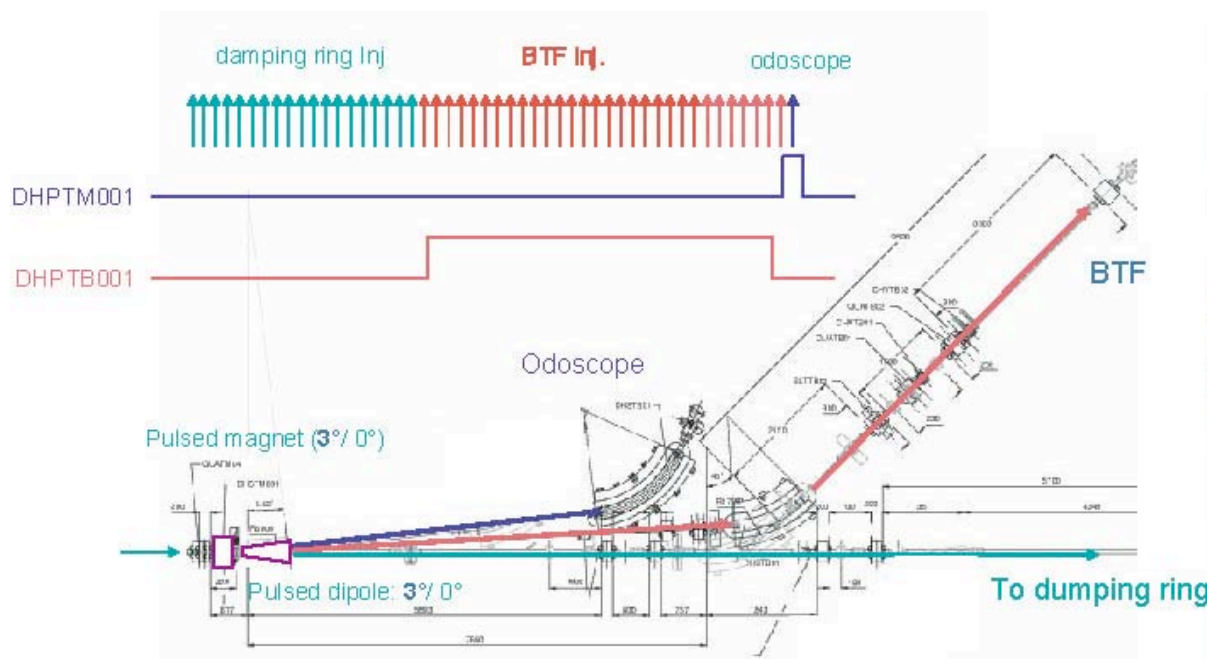

Figure 27 - The DANAE BTF Injection scheme: a pulsed magnet intercepts the high current electron/positron beam coming from the LINAC at 50 Hz bending ≤ 30 of the incoming pulses into the BTF transfer line. Whenever needed for monitoring, one pulse can be also deviated to the hodoscope for energy measurement.

The maximum operation energy, when working in DANAE-BTF mode, is limited by the impossibility to change in a fast way the LINAC energy settings, fixed at 510 MeV for injection in the damping ring.

In conclusion, some modifications must be done in order to operate the Beam Test Facility in the new injection scheme. The parameters of operation when injection in the damping ring is off does not change with respect to the present situation, while in the DANAE-BTF operation mode only the energy range and repetition frequency are limited.

The parameter list of BTF is shown in Table XIV.

Table XIV - BTF parameters list

Operation/parameter	BTF only mode	DANAE-BTF mode
Energy Range	25-750 MeV	25-510 MeV
Repetition Rate	50 Hz	>30 Hz[*]
Up time	100%	90-100%
Current/pulse	1 to 10^{10}	
Pulse Duration	1 or 10 ns	
Energy resolution	1 %	
Spot size	$\sigma_x \sim \sigma_y \sim 2$ mm[**] -1 cm	
divergence	2[**]–15 mrad	

[*] train of contiguous pulses with a separation of 20 ms and a repetition rate of 1Hz.
[**] single particle mode

Synchrotron radiation lines

DAΦNE is presently used in parasitic mode as a synchrotron radiation source [44]. This facility can be maintained in the DANAE ring, where the light can be extracted both from the dipoles and from the wigglers. A Letter of Intent of the LNF synchrotron radiation group is being prepared [45].

The proposed layout (see Fig. 1) is compatible with some of the existing lines. The positron ring is proposed as the light source, because the positron beam emittance does not suffer from ion trapping. Anyway, with the proposed new injection transfer lines, and at this stage of the project, the beams can be interchanged with no major modifications.

Table XV summarizes the set of parameters of interest for the synchrotron radiation source.

Table XV – Parameters of DANAE as a possible synchrotron radiation source.

Energy (GeV)	0.51	1.2
I (A)	2.5	0.5
Number of bunches	150	30
Beam lifetime (sec)	1000	7000
Time between injection (min)	5	60
Bunch spacing (nsec)	2	10
Horizontal emittance (mm mrad)	0.45	0.45
Vertical emittance (mm mrad)	0.002	0.002
B @dipoles	0.72	1.73
λ_c (A°) @dipoles	100	7
B @wigglers	4	4
λ_c (A°) @wigglers	18	3

RADIATION SHIELDING

An evaluation of the necessary additional shielding for DANAE operation has been done. The same radiation shielding must be used for both operation modes, the one at low energy and high current (510 MeV, 2.5A), and the one at low current and high energy (1200 MeV, 600 mA), operation modes that will be alternated with periods of the order of years.

Let's summarizes the characteristics of the two operation conditions from the point of view of radiation shielding:

510 MeV:
>*Standard injection in the Damping Ring*
>e^- 100mA 50 Hz 10ns beam loss 5%
>e^+ 40 mA 50Hz 10ns beam loss 10%
>injection time per year: 1800 hours/beam
>*Standard injection cycle in DANAE*
>e^- 150 pulses 1 Hz 500ps beam loss 5%
>e^+ 150 pulses 1 Hz 500ps beam loss 5%
>300 s of pause
>*Number of injections per year*
>144 injections per day per beam x300 working day/year =
>43200 injections per year per beam=1800 h per year per beam
>*Beam losses on stored beam*
>0.5A/5' = 1.7 x $10^9 e^-$/s
>with the hypothesis of targets used for beam stopping, ad hoc installed

1200 MeV
>*Standard injection cycle in DANAE*
>e^- 150 pulses 1 Hz 500ps 5% losses
>e^+ 150 pulses 1 Hz 500ps 5% losses
>4300 s of pause
>*Beam losses on stored beam*
>0.3A /75'= $1.36 \times 10^8 e^-$/s
>with the hypothesis of targets used for beam stopping, ad hoc installed
>*Lost beam by kicker (dumped)*
>0.3A /75'

The constraint on the ambient dose equivalent H*(10) 1 mSv/year and on the effective dose for areas outside shields is below few μSv/h.

Damping Ring shielding needs:
- Lateral shield not less than 140 cm concrete (already existing);

and, if not already installed
- 20 cm Pb externally to the injection septa and to all bending magnets of the half ring comprised between the direction e- and e+;
- Roof shield no less 50 cm concrete (already existing);
- 15 cm of iron (already existing, magnets and other magnetic components),

and, if not already installed
- 5 cm Pb and 20 cm concrete on the injection septa and to all bending magnets of the half ring comprised between the direction e- and e+.

In addition to the actual DAΦNE shield DANAE shielding needs:
- Shield of main hall windows not less 50 cm concrete;
- Injection septa lateral shields 15 cm Pb;
- Injection septa forward shields 30 cm Pb;
- Injection septa roof shield 10 cm Pb plus 50 cm concrete;
- Same kind of shielding around points of targets installed to absorb beam losses;
- Installation of a beam dump for beam killed by kicker.

These shields reduce neutron skyshine to negligible values.

Photon skyshine is some orders of magnitude less than the neutron one.

SCHEDULE and COSTS

A preliminary schedule of the project is shown in table XVI.

Table XVI – Schedule for DANAE project

	T0+1 year			T0+2 years			T0+3 years			T0+4 years		
Project - Drawings - Tender request	■	■	■	■	■	■						
Realization				■	■	■	■	■	■			
DAΦNE Decommissioning							■					
Buildings Modification							■	■				
Installation								■	■	■	■	
Commissioning										■	■	■

T_0 corresponds to the moment of project approval. The time needed for the technical design of all components and preparation of the calls for tenders is 18 months, and the same time is needed for the construction, although there is some overlap between the two items.

The first two years of the project overlap with DAΦNE operation for experiments. Once completed the DAΦNE program, the Main Ring components can be decommissioned, and at the same time the necessary building modifications for the new transfer lines can be done. There is also the possibility of making these modifications and the first part of the transfer lines in a previous DAΦNE shutdown, so that the upgrade of the injection system is already effective for the last DAΦNE runs. In fact the first part of the lines, up to the DAΦNE hall, are compatible with the DAΦNE injection system (see Fig. 1).

The decommissioning time has been estimated as 3 months, considering that only the components inside the DAΦNE hall must be disinstalled. One year is estimated for the two rings installation, and nine months for commissioning.

The total time from the project approval to the collisions for the first experiment is therefore 4 years.

The cost of the total project has been estimated on the basis of the most recent available technology at today prices and a contingency of 10% has been added for a more conservative evaluation, and the details and total sum are given in Table XVII.

Table XVII – Costs of the DANAE project

	Number	Cost per unit €	Total Cost €	Total € with 10% contingency
Dipoles	24	68000	1632000	1795200
Quadrupoles	0	21000	0	0
SC Quadrupoles	6	60000	360000	396000
Sextupoles	8	21000	168000	184800
Correctors	10	11000	110000	121000
Longitudinal and transverse feedback kickers	8	30000	240000	264000
Injection kickers	0	300000	0	264000
Wigglers SC 3*2m*4T	4	1200000	4800000	5280000
Injection Transfer Lines	2	500000	1000000	1100000
Ring vacuum chambers	4	1000000	4000000	
Interaction region vacuum chamber	2	360000	720000	5192000
Power Supplies				
• Quadrupoles	0	35000	0	
• Sextupoles	8	26000	208000	
• Correctors	10	11000	110000	
• SC Quadrupoles	18	10000	180000	
• Wiggler SC	8	26000	208000	
• Splitters	0	140000	0	846600
RF				
Main cavities with power source	2	1600000	3200000	
Crab cavities with power source	2	500000	1000000	4620000
Control system	1	4000000	4000000	4400000
Feedbacks	8	60000	480000	528000
Diagnostics	1	1700000	1700000	1870000
Cryogenics				
Cryocooler	6	35000	210000	
Transfer Lines	2	25000	50000	
Plant TCF50 upgrade	1	2400000	2400000	2926000
Installation	1	600000	600000	660000
Fluids	1	300000	300000	330000
Linac restyling	1	2000000	2200000	2200000
Electric plant	1	300000	300000	330000
Building modifications for transfer lines	1	300000	300000	330000
Total				33373600

REFERENCES

1. "Proposal for a Φ-Factory", Laboratori Nazionali di Frascati-INFN, LNF-90/31(R), pp. 325-371 (1990).
2. "KEKB B-factory Design report", KEK Report 95-1, (1995).
3. "PEP-II An Asymmetric B-Factory, Conceptual Design Report", SLAC Report 418 (1993).
4. Conceptual Design Report of BEPC II (March 2001).
5. Yu M. Shatunov et al.: "Project of a New Electron-Positron Collider VEPP-2000", Proc. of EPAC 2000, Vienna (2000).
6. KLOE Collaboration: "KLOE: A General Purpose Detector for DAΦNE", Laboratori Nazionali di Frascati-INFN, LNF-92/019 (IR), (1992).
7. FINUDA Collaboration: "Finuda Technical Report", Laboratori Nazionali di Frascati-INFN, LNF-95/024 (IR), (1995).
8. DEAR Collaboration: "DAΦNE Exotic Atom Research - DEAR Proposal", Laboratori Nazionali di Frascati-INFN, LNF-95/055 (IR), (1995).
9. "Expression of Interest for the continuation of the KLOE physics program at DAΦNE upgraded in luminosity and in energy", in preparation.
10. F. Ambrosino et al.: "Prospects for e+e- physics at Frascati between the Φ and the Ψ", in preparation.
11. "Measurement of the nucleon form factor in the time-like region at DAΦNE2", http://www.lnf.infn.it/conference/nucleon05/FF/
12. "LoI for the study of deeply bound kaonic nuclear states at DAΦNE", in preparation.
13. ILC − International Linear Collider, http://www.linearcollider.org/cms/
14. "Workshop on e+ e- in the 1-GeV to 2-GeV Range: Physics and Accelerator Prospects - ICFA Mini-workshop - Working Group on High Luminosity e+ e- Colliders", Alghero, Sardinia, Italy, 10-13 September 2003, http://www.lnf.infn.it/conference/d2/
15. A. Gallo, P. Raimondi and M. Zobov, "Strong RF Focusing for Luminosity Increase: Short Bunches at IP", e-Print Archive: physics/0404020; C. Biscari, "Bunch Length Modulation in Highly Dispersive Storage Rings", Phys. Rev. ST Accel. Beams 8: 091001, 2005.
16. D. Alesini, G. Benedetti, M.E. Biagini, C. Biscari, R. Boni, M. Boscolo, B. Buonomo, A. Clozza, G. Delle Monache, G. Di Pirro, A. Drago, A. Gallo, A. Ghigo, S. Guiducci, M. Incurvati, C. Ligi, F. Marcellini, G. Mazzitelli, C. Milardi, L. Pellegrino, M.A. Preger, L. Quintieri, P. Raimondi, R. Ricci, U. Rotundo, C. Sanelli, M. Serio, F.Sgamma, B. Spataro, A.Stecchi, A.Stella, S. Tomassini, C. Vaccarezza, M. Vescovi, M. Zobov: "Preliminary Considerations on Machine Requirements for a Neutron-Antineutron Form Factor Experiment at Frascati", LNF-DAΦNE Technical Note, G-63, 15/7/2005, http://www.lnf.infn.it/acceleratori/dafne/NOTEDAFNE/G/G-63.pdf
17. D. Boussard, "Observation of microwave longitudinal instabilities in the CPS", LABII/RF/Int./75-2, 24 April 1975.
18. R.H. Helm, M.J. Lee, P.L. Morton, M. Sands, "Evaluation of Synchrotron Radiation Integrals", IEEE Trans. Nucl. Science, NS 20, 900 (1973).
19. DAΦNE Machine Development Shift on 13/04/2005: http://www.lnf.infn.it/acceleratori/dafne/report/High_momentumCompaction.pdf
20. B.V. Podobedov, "Saw Tooth Instability Studies at the Stanford Linear Collider Damping Rings", Ph.D. Thesis, SLAC-R-543, June 1999.

21. A. Drago et al., "Longitudinal Quadrupole Instability and Control in the Frascati DAΦNE Electron Ring", Rhys.Rev. ST Accel.Beams 6: 052801, 2003.

22. A. Temnykh, "Effect of High Synchrotron Tune on Beam-Beam Interaction: Simulation and Experiment", Talk presented at ICFA Mini-Workshop on "Frontiers of Short Bunches in Storage Rings", 7-8 November 2005, 2005, Frascati, Italy:
http://www.lnf.infn.it/conference/sbsr05/TALKS/temnikh.ppt
A. Temnykh: "CESRc Wiggler Magnets", ICFA Mini-workshop – Working Group on High Luminosity e+e- Colliders, 10-13 September 2003, Alghero (SS), Italy,
http://www.lnf.infn.it/conference/d2/TALKS/Temnykh2.pdf

23. M. Zobov, "Negative Momentum Compaction at DAΦNE", Talk presented at the Workshop "e+e- in the 1-2 GeV Range: Physics and Accelerator Prospects", 10-13 September 2003, Alghero, Italy:
http://www.lnf.infn.it/conference/d2/TALKS/zobov1.pdf

24. K. Hosoyama, K. Hara, A. Kabe, Y. Kojima, Y. Morita, H. NakaiI, Li Shao Peng, K. Ohkubo, H. Hattori and M. Inoue, "Superconducting Crab Cavity for KEKB", proc. of the 1998 APAC, Tsukuba.

25. B. Parker, J. Escallier, "Serpentine coil topology for BNL direct wind superconducting magnets", Proc. of 2005 Part. Acc. Conf., Knoxville, USA, May 2005, pg. 737.

26. M. Biagini, C. Biscari: "Tunable Interaction Region for DAFNE Upgrade", LNF-DAΦNE Technical Note, IR-13, 29/7/2005,
http://www.lnf.infn.it/acceleratori/dafne/NOTEDAFNE/IR/IR-13.pdf

27. S.A. Nikitin for VEPP-2M Team, "Present Activities at Colliders of BINP (Novosibirsk)", in Proceedings of International Workshop on Performance Improvement of Electron-Positron Collider Factories "e+e- Factories'99", KEK, Tsukuba, Japan, 1999. KEK Proceedings 99-24: 37-44, 2000.

28. M. Zobov et al., "Bunch Lengthening and Microwave Instability in the DAΦNE Positron Ring", e-Print Archive: physics/0312072.

29. M. Boscolo, M. Antonelli, S.Guiducci, "Simulations and measurements of the Touschek background at DAΦNE", EPAC02, Paris, France, 2002.

30. T. Tajima, K. Akai, E. Ezura, T. Furuya, K. Hosoyama, S. Mitsunobu, "The Superconducting Cavity System for KEKB", proc. of the 1999 PAC, New York.

31. D. Teytelman, C. Rivetta, D. Van Winkle, R. Akre, A. Drago, J. Flanagan, J. Fox, A. Krasnykh, T. Naito, M. Tobiyama, "Design and testing of Gproto bunch-by-bunch signal processor ", abstract presented at EPAC06

32. R. Boni, A. Gallo, A. Ghigo, F. Marcellini, M. Serio, M. Zobov: "A Waveguide Overloaded Cavity as Longitudinal Kicker for the DAΦNE Bunch-by-Bunch Feedback System", Particle Accelerators, 1996, Vol. 52, pp. 95-113, 1996.

33. F. Marcellini, M. Tobiyama, P. McIntosh, J. Fox, H. Schwarz, D. Teytelman, A. Young: "Study and Design of a New Over-damped Cavity Kicker for the PEP II Longitudinal Feedback System", presented at BIW2002, 6-9 May 2002, BNL, New York, USA; AIP Conference Proceedings, Vol. 648, 458-466 (2002).

34. J. Irwin et al.: "Model-Independent Beam Dynamics Analysis", Phisical Review Letters, Vol 82, 8, 2-22-1999 (1999).

35. D.Teytelman, Private communication.

36. S. Prabhakar: "New Diagnostics and Cures for Coupled-Bunch Instabilities", SLAC Report SLAC-R-554 (UC-410), (2000).

37. G. Di Pirro, G. Mazzitelli, I. Sfiligoi, A. Stecchi: "The Evolution of ohe DAΦNE Control System: A History of Liberation from Hardware", ICALEPCS 2001, San Jose,

California, 27-30 November 2001; San Jose 2001, Accelerator and large experimental physics control systems, 222-224.

38. M. Zobov et al.:" Collective effects and impedance study for the DAΦNE Phi-Factory", Proceedings of the International Workshop on Collective Effects and Impedance for B-Factories, Tsukuba, Japan, 12-17 June, 1995, http://www.lnf.infn.it/acceleratori/dafne/PUBLICATIONS/ZOBOV_KEK95.pdf LNF-95-041(P), 31/07/1995.

39. "CTF3 Design Report" edited by G. Geschonke and A. Ghigo, CERN/PS 2002-008 (RF), LNF-02/008 (IR).

40. C. Vaccarezza: "Ion Trapping Effect and Clearing in the DAΦNE Main Electron Ring", LNF-DAΦNE Technical Note G-38, 27/5/1996, http://www.lnf.infn.it/acceleratori/dafne/NOTEDAFNE/G/G-38.pdf

41. S. Kulinski, R. Boni, B. Spataro, M. Vescovi: "The Linear Accelerator for the DAΦNE Injection System", LNF - DAΦNE Technical Note LC-1, 11/2/1991, http://www.lnf.infn.it/acceleratori/dafne/NOTEDAFNE/LC/LC-1.pdf

42. D. Alesini: "Fast Injection Kickers for DAΦNE and ILC Damping Rings", LNF-DAΦNE Technical Note to be published.

43. G. Mazzitelli, A. Ghigo, F. Sannibale, P. Valente, G. Vignola: "Commissioning of the DAFNE Beam Test Facility", Nuclear Instruments & Methods in Physics Research A 515 (2003) 524-542; LNF-03/003(P), 24/02/03, http://www.lnf.infn.it/sis/preprint/pdf/LNF-03-3%28P%29.pdf

44. DAΦNE-LIGHT, LNF–Synchrotron Radiation Facility, http://www.lnf.infn.it/esperimenti/sr_dafne_light/

45. A. Balerna, M. Benfatto, M. Cestelli-Guidi, R. Cimino, A. Grilli, S. Mobilio, M. Piccinini: "DANAE as a synchrotron radiation source", in preparation.